Heliyon

Received:
2 September 2017
Revised:
3 January 2018
Accepted:
11 January 2018

Cite as: Mads N. Olesen, Josefine R. Christiansen, Steen Vang Petersen, Poul Henning Jensen, Wojciech Paslawski, Marina Romero-Ramos, Vanesa Sanchez-Guajardo. CD4 T cells react to local increase of α-synuclein in a pathology-associated variant-dependent manner and modify brain microglia in absence of brain pathology. Heliyon 4 (2018) e00513. doi: 10.1016/j.heliyon.2018.e00513

CD4 T cells react to local increase of α-synuclein in a pathology-associated variant-dependent manner and modify brain microglia in absence of brain pathology

Mads N. Olesen [a,b,1], **Josefine R. Christiansen** [a,b,c,2], **Steen Vang Petersen** [d], **Poul Henning Jensen** [e], **Wojciech Paslawski** [f,3], **Marina Romero-Ramos** [b,c], **Vanesa Sanchez-Guajardo** [a,b,*]

[a] *Neuroimmunology of Degenerative Diseases Group, Department of Biomedicine, Aarhus University, Aarhus, Denmark*

[b] *AUideas Pilot Center NEURODIN, Department of Biomedicine, Aarhus University, Aarhus, Denmark*

[c] *CNS Disease Modeling Group, Department of Biomedicine, Aarhus University, Aarhus, Denmark*

[d] *Laboratory for Redox Regulation, Department of Biomedicine, Aarhus University, Aarhus, Denmark*

[e] *DANDRITE, Department of Biomedicine, Aarhus University, Aarhus, Denmark*

[f] *iNANO, Department of Molecular Biology and Genetics, Aarhus University, Aarhus, Denmark*

* Corresponding author.

E-mail address: vamasag@mac.com (V. Sanchez-Guajardo).

[1] Current address: Department of Clinical Biochemistry and Immunology, Vejle Hospital, Vejle, Denmark.

[2] Current address: Center for Basic and Translational Neuroscience, University of Copenhagen, Copenhagen N, Denmark.

[3] Current address: Department of Clinical Neuroscience, Karolinska Institute, Stockholm, Sweden.

Abstract

We have previously shown that immunological processes in the brain during α-synuclein-induced neurodegeneration vary depending on the presence or absence of cell death. This suggests that the immune system is able to react differently to the different stages of α-synuclein pathology. However, it was unclear whether these immune changes were governed by brain processes or by a direct immune

http://dx.doi.org/10.1016/j.heliyon.2018.e00513

response to α-synuclein modifications. We have herein locally increased the peripheral concentration of α-synuclein or its pathology-associated variants, nitrated or fibrillar, to characterize the modulation of the CD4 T cell pool by α-synuclein and brain microglia in the absence of any α-synuclein brain pathology. We observed that α-synuclein changed the CD4:CD8 ratio by contracting the CD3+CD4+ T cell pool and reducing the pool of memory Regulatory T cells (Treg). Nitrated α-synuclein induced the expansion of both the CD3+CD4+ and CD3+CD4− T cells, while fibrils increased the percentage of Foxp3+ Treg cells and induced anti-α-synuclein antibodies. Furthermore, the activation pattern of CD3+CD4+ T cells was modulated in a variant-dependent manner; while nitrated and fibrillar α-synuclein expanded the fraction of activated Treg, all three α-synuclein variants reduced the expression levels of STAT3, CD25 and CD127 on CD3+CD4+ T cells. Additionally, while monomeric α-synuclein increased CD103 expression, the fibrils decreased it, and CCR6 expression was decreased by nitrated and fibrillar α-synuclein, indicating that α-synuclein variants affect the homing and tolerance capacities of CD3+CD4+ T cells. Indeed, this correlated with changes in brain microglia phenotype, as determined by FACS analysis, in an α-synuclein variant-specific manner and coincided in time with CD4+ T cell infiltration into brain parenchyma. We have shown that the peripheral immune system is able to sense and react specifically to changes in the local concentration and structure of α-synuclein, which results in variant-specific T cell migration into the brain. This may have a specific repercussion for brain microglia.

Keywords: Neuroscience, Immunology

1. Introduction

Parkinson's disease (PD) is characterized by the loss of dopaminergic neurons in substantia nigra and the presence in surviving neurons of pathological α-synuclein (α-syn) aggregates termed Lewy bodies. α-syn is ubiquitously expressed in neurons, but also in erythrocytes and in most immune cells (Barbour et al., 2008; Sanchez-Guajardo et al., 2013; Shin et al., 2000). Growing evidence suggest that α-syn released from cells, both unfolded and misfolded, can be uptaken by neighboring cells. The misfolded uptaken α-syn would then induce other α-syn to change conformation, promoting pathological aggregation and cellular degeneration. This spreading process has been postulated to occur in PD, with the peripheral nervous system as an entrance of the pathological α-syn to the CNS (reviewed in Goedert, 2015). During this process the immune system would play a central role in the handling and clearance of extracellular α-syn, as well as in the maintenance and protection of neurons. The peripheral immune system is in constant contact with α-syn, as it is present in serum due to its release from cells (Desplats et al., 2009; Lee et al., 2012; Luk et al., 2012). Additionally, lymphocytes and other immune cells express themselves α-syn (Shin et al., 2000) and accumulate it with

http://dx.doi.org/10.1016/j.heliyon.2018.e00513

age (Gardai et al., 2013; Kim et al., 2004). It is becoming apparent that an α-syn immune response is important for brain processes. It has been related to immune response to virus in brain (Beatman et al., 2015) Also, α-syn knockout mice show impaired B cell development and IgG production (Xiao et al., 2014), as well as a decrease in T cells and a defective Th2 phenotype in CD4+ cells (Shameli et al., 2016).

Numerous studies have addressed the effect α-syn has on microglia and how this affects the brain (reviewed in Sanchez-Guajardo et al., 2013) but little is known about the effect that α-syn and its possible modifications have on the peripheral immune system.

Studies of the T cell population in PD patients suggest changes in the peripheral adaptive immune system, in particular the CD4 compartment (Bas et al., 2001; Gruden et al., 2011; Stevens et al., 2012). Contradictory changes have been reported regarding the decrease of the regulatory CD4 T cell (Treg) compartment as compared to healthy subjects (Baba et al., 2005; Saunders et al., 2012), but PD-derived Treg cells (CD4+CD25+CD127−) *ex vivo* have reduced suppressive activity (Saunders et al., 2012). However, ageing studies have reported that Treg absolute numbers increase with age, even in PD (Rosenkranz et al., 2007; Wang et al., 2010).

Notably, T cells express dopamine receptors (DRs) and the dopamine transporter (Saha et al., 2001). Thus, the characteristic decrease in dopamine found in PD may also be sensed by and/or affecting the T cell population. Indeed in PD, DR changes on T cells have been observed (Kustrimovic et al., 2016; Nagai et al., 1996). The type of DR expressed by the T cell and the presence/absence of dopamine influence the type of effector cell a CD4 T-cell differentiates into (*i.e.* Th1 *vs.* Th2) (reviewed in Pacheco et al., 2009).

α-syn is present in serum; however, it is unclear how this changes during PD as data exists showing both increase (Lee et al., 2006) and decrease (Mollenhauer, 2014) of α-syn in serum. Anyhow, anti-α-syn antibodies are found in patients' serum suggesting a sterile immune response in PD (Besong-Agbo et al., 2013; Maetzler et al., 2011; Papachroni et al., 2007). Sterile immune responses have been observed in Alzheimer's disease and relate to early non-T cell receptor (TCR)-mediated responses that result in inflammation in the absence of a pathogen. One could thus postulate that changes in concentration or modification of α-syn could trigger a similar immune responses during PD. Therefore, discerning how the peripheral immune system reacts to changes in α-syn is of vital interest if we want to elucidate the role, if any, the peripheral immune system plays in PD. This knowledge will further help to develop effective immunoregulatory therapies for PD, as T cells may not be responding the same way as in healthy conditions.

http://dx.doi.org/10.1016/j.heliyon.2018.e00513

In light of this, we aimed to elucidate how, and if, the peripheral adaptive immune system, in particular CD4 T cells, reacts to local peripheral increases in α-syn, an autologous protein to which the immune system should be tolerant (*i.e.* unresponsive). We also studied whether the CD4 T cell pool is modulated by different PD pathology-associated variants of α-syn (nitrated and fibrillar α-syn), as this could give insight into how the peripheral immune system regulates its response as pathology progresses. Lastly, we have studied whether these α-syn induced changes in the peripheral immune system have any influence in brain microglia.

2. Material and methods

2.1. Animals & inoculation strategy

A total of 48 ten-week-old Foxp3-IRES-mRFP (FIR) reporter mice (Wan and Flavell, 2005) (C57BL/6 background; a kind gift from Prof. Antonio A. Freitas, Pasteur Institute, France) were equally distributed between sexes and divided into five experimental groups (n = 8–10/group). There were no detectable differences due to animal gender throughout the project, as determined by direct comparison of the results when separated by gender, which gave quasi-equal average and standard deviation (SD). Our inoculation strategy consisted of 100 μg protein administered subcutaneously at the base of the tail in a total volume 300 μl isotonic saline. After four weeks the animals were again injected with the same amount of protein and subsequently euthanized five days later for analysis.

The proteins used were recombinant human monomeric α-syn, its nitrated or its fibrillar form, as these pathology-associated modifications are known to exacerbate brain pathology. No adjuvant was used during the inoculation, since our aim was to mimic the accumulation of α-syn due to pathology and not to induce a vaccination type of reaction. A group of naïve animals was included to determine the baseline of all immunological parameters, such as cell numbers, percentage, and distribution of cell populations and activation states. Additionally, we included a group of animals inoculated with LPS (10,000 EU/g, Sigma-Aldrich, St. Louis, MO) to determine the specificity of the α-syn-induced changes as compared to this well-established pro-inflammogen. LPS inoculation took place at the time of the second inoculation with α-syn or its variants. The animals from the five experimental groups were distributed into 3–4 independent experiments. Animal permits to perform the experiments were approved by the Animal Experiments Inspectorate. All experimental animal work was conducted according to Danish regulations (Law no. 253, 08 03 2013, Executive order no. 88, 30 01 2013) in agreement with European Union directive (2010/63/EU) and under the guidance of the veterinarian of the Health Faculty, Aarhus University.

http://dx.doi.org/10.1016/j.heliyon.2018.e00513

2.2. Protein preparations

Human recombinant α-syn was prepared as described (Nielsen et al., 2013). A fraction of α-syn was nitrated following the protocol from Reynolds et al. (2010), and nitration was subsequently verified by western blot (≥98% of total α-syn) and mass spectrometry. Purified α-syn and nitrated α-syn was diluted in 50 mM ammonium bicarbonate and digested overnight at 37 °C using porcine trypsin (Promega Biotech AB, Sweden) at a 1:40 ratio. The samples were subsequently lyophilized, resuspended in 0.1% formic acid (FA) and analyzed by LC–MS/MS by using an Ultimate 3000 system (Thermo Scientific, Carlsbad, CA, USA) connected to a MicroTOF-Q II mass spectrometer (Bruker Dalton, MA, USA). The peptides were recovered using an Acclaim PepMap100 column (75 μm ID, 15 cm length) and eluted by a linear gradient of solvent B (90% acetonitrile, 0.08% (v/v) FA) in solvent A (0.1% (v/v) FA) from 5% to 50% with a flow rate of 200 nl min^{-1}. The obtained mass spectra (MGF-files) were searched against the Swiss-Prot *Homo sapiens* database as reference (2016_08) using the Mascot 2.5 search engine. Search parameters were set to allow for one missed cleavage, and oxidation of methionine and nitration of tyrosine as variable modifications. The mass tolerances of the precursor and product ions were 20 ppm and 0.8 Da, respectively. The cleavage of human α-syn by trypsin generates a peptide encompassing Tyr39 (Glu34-Lys42; 950.5 Da) and a larger peptide encompassing Tyr125, 133, and 136 (Asn103-Ala140; 4285.7 Da). The size of the latter does not allow for adequate detection by LC-MS/MS. The MS/MS analysis showed that the peptide encompassing Tyr39 was unmodified in the control sample whereas the nitrated peptide was detected in the derivatized α-syn sample, as indicated by the presence of specific product ions (Fig. 1). Additionally, the unmodified Glu34-Lys42 peptide was not detected in the nitrated sample indicating a high degree of nitration of Tyr39.

Fibrillar α-syn was prepared as described (Lindersson et al., 2004). The state of fibrillation was determined by Thioflavin T Fluorescence Assay, samples were taken at different time points during the fibrillation process and fluorescence measurements were performed at final concentrations of 10 μg protein and 20 μg thioflavin T in 90 mm glycine-NaOH, pH 8.5, using a Wallac Victor^3 1420 (PerkinElmer Life Sciences, MA, USA) multilabel counter (excitation at 450 nm, emission at 486 nm) with 1-s integration. The obtained measurements were (counts, AU): Fibrils: 14174, monomer: 685, and background: 791. Additionally a sedimentation assay was performed, where a fraction of the filament preparation prior to freezing was subjected to centrifugation and split in pellet and supernatant. The preparation was approximately 70–80% insoluble. All data concerning the characterization of the fibrils used in here have been previously published (Lindersson et al., 2004). All protein solutions stocks were kept at 1 μg/μl in isotonic saline, and at the time of injection diluted in isotonic saline to obtain a volume of 300 μl/mouse of protein solution.

http://dx.doi.org/10.1016/j.heliyon.2018.e00513

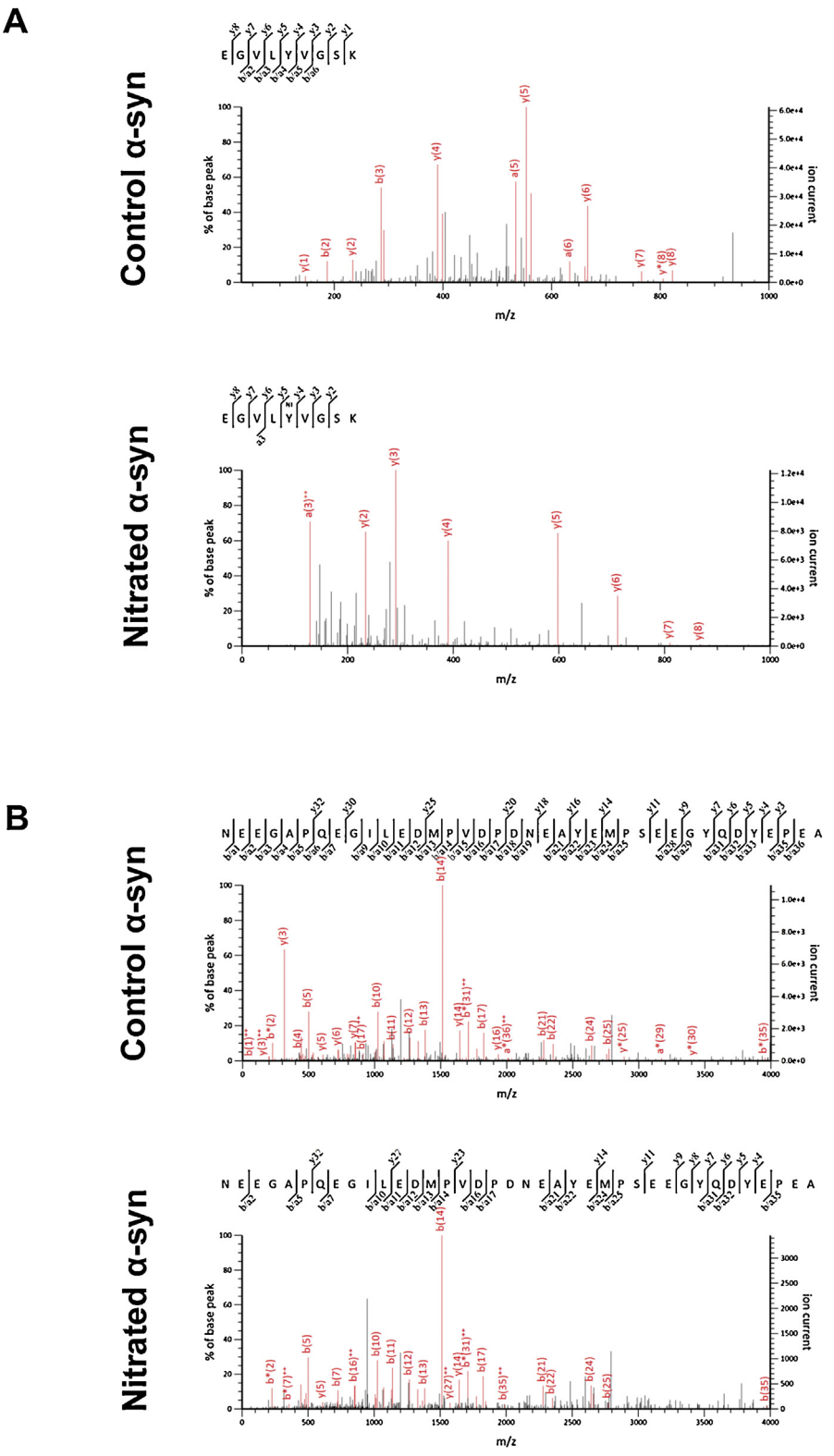

Fig. 1. Characterization of the nitration of α-syn. MS/MS spectra representing the fragmentation of the Glu34-Lys42 precursor ion. The spectra of the generated product ions were extracted from the Mascot software. Spectra show that Tyr39 is indeed nitrated in the derivatized α-syn sample (A) whereas the peptide encompassing Tyr125, 133, and 136 was found unmodified in the derivatized sample (B).

http://dx.doi.org/10.1016/j.heliyon.2018.e00513

2.3. Lymph node cell preparation

At time of death, the inguinal, axillar and brachial lymph nodes were pooled per animal and single cell suspensions were made in complete medium (RPMI 1640-GlutaMax, with 10% FCS, HEPES and penicillin/streptomycin, all from Invitrogen, Carlsbad, CA, USA). Cells were filtered through a 100 μm mesh and washed in 10 ml medium. After centrifugation (400*g* for 10 min), the cells were resuspended in 1 ml complete medium. An aliquot was taken for cell counting and 100 μl were taken for flow cytometry analysis. The remaining cells were plated on round bottom plates and let to rest in an incubator for 6 h, after which the medium was recovered, and the cells were lysed in complete lysis buffer (1 cOmplete Mini protease inhibitor tablet and 2phosSTOP tablets (both Roche Diagnostics, Basel, Switzerland) per 10 ml lysis buffer: 10 mM Tris-base, 150 mM NaCl, 0.5 mM EDTA, 1% IGEPAL CA-630 in deionized water). Both samples were frozen at −20 °C until further analysis.

2.4. Microglia isolation

Brains were quickly dissected at the time of death and homogenized in 1.4 ml of HBS medium (Invitrogen); 600 μl of trypsin (50 mg/ml, Trypsin-EDTA, Sigma-Aldrich, St. Louis, MO, USA) were added, and the mix was put on a 37 °C water bath for 15 min. Two ml HBS medium and 800 μl of FCS (20%) were added before centrifugation (200*g* for 4 min). The pellet was resuspended in 5 ml HBS and carefully pipetted to obtain a single cell suspension. The sample was filtered (40 μm) before centrifugation, and the pellet was resuspended in 2.3 ml 75% Percoll (GE Healthcare, Uppsala, Sweden). Five ml of 25% Percoll followed by 3 ml PBS were layered on top of the cell suspension, and the sample was centrifuged for 25 min at 800*g*. Microglia were recovered from the interphase between the 75–25% gradient and washed with 15 ml PBS. After centrifugation, the pellet was resuspended in 100 μl PBS for FACS analysis.

2.5. Flow cytometry

All samples were plated on a 96 conical well plate and centrifuged 4 min at 400*g*. The cells were then incubated 10 min with 30 μl/well Fc block, centrifuged again, and resuspended in 30 μl antibody mix (for antibody specifications see Table 1) for 10 min incubation in the dark. After washing, 30 μl/well of secondary antibody mix was added, and the cells were further incubated for 10 min in the dark, washed twice, and resuspended in 200 μl buffer. All incubations were done on ice, and all the washes (100 μl, 300 g) and antibody mix were done in PBS with 0.5 mM EDTA, penicillin/streptomycin, 2% FCS without Ca^{2+} and Mg^{2+}. Sample data was acquired in a FACS ARIA III (with 4 lasers) interphased to FlowJo software for analysis. All samples were gated first on live cells according to their FSC *vs.* SSC,

http://dx.doi.org/10.1016/j.heliyon.2018.e00513

Table 1. List of antibodies used.

Antibody	Coupled to	Dilution	Made in	Clone	Manufacturer	Function
Flow cytometry						
CD4	AF700	1:800	Rat	RM4-5	BD Pharmingen	TCR complex, binds MHC-II
CD3ε	HV500	1:100	Syrian Hamster	500A2	BD Horizon	TCR complex, kinase
CD25	PE-Cy7	1:200	Rat	PC61	BD Pharmingen	IL-2Rα, T cell activation/Treg survival
DR-D2	Purified	1:50	Goat	Polyclonal	Abcam	Dopamine receptor D2
DR-D3	Purified	1:50	Rabbit	Polyclonal	Abcam	Dopamine receptor D3
CD127	Biotin	1:100	Rat	A7R34	eBioscience	IL-7Rα, effector/memory T cell
CD196 (CCR6)	BV421	1:50	Armenian Hamster	29-2L17	Biolegend	CCR6Chemokine receptor. Migration & homeostasis of lymphocytes.
CD103	PerCP-Cy5.5	1:100	Armenian Hamster	2E7	BioLegend	Lectin, tolerance. Treg express high levels. Th cells use it to attach to endothelium and extravasate
CD11b	PE-Cy7	1:800	Rat	M1/70	BD Pharmingen	Lectin, binds ICAM-1. When in complex with CD18, forms CR3 (binds C3bi). Macrophage/monocyte cells
CD11c	AF700	1:800	Armenian Hamster	N418	BioLegend	Lectin, When in complex with CD18, forms CR3 (binds C3bi). Dendritic & NK cells
CD54 (ICAM-1)	APC	1:100	Hamster	3E2	BD Pharmingen	ICAM-1, binds CD11b/CD18 & CD11c/CD18, involved in MHC-II-independent responses to weak immunogenic tumor cells
CD154 (CD40L)	Biotin	1:50	Armenian Hamster	MR1	BD Pharmingen	CD40 ligand, binds CD40. Normally associated to lymphocytes, it is widely expressed on other types of cells (Schonbeck and Libby, 2001).
CD200R	PE	1:200	Rat	OX-110	Biolegend	Ox-2R, Suppresses inflammatory reactions on macrophages, Neuron-glia inhibitory interaction
MHC-II (I-A/I-E)	eFluo450	1:100	Rat	M5/114.15.2	eBioscience	Antigen presentation, binds CD4/TCR
CD172a	FITC	1:100	Rat	P84	BD Pharmingen	Adhesion molecule. Neurons, retina macrophages. Regulates phagocytosis and synaptic activity. Microglia-neuron regulatory interactions.

(*Continued*)

http://dx.doi.org/10.1016/j.heliyon.2018.e00513

Table 1. (*Continued*)

Antibody	Coupled to	Dilution	Made in	Clone	Manufacturer	Function
CD4	APC-H7	1:200	Rat	GK1.5	BD Pharmingen	TCR complex, binds MHC-II
Streptavidin	QDot605	1:200				Secondary antibody
Anti-rabbit IgG	AF647	1:100	Donkey	n.a.	Abcam	Secondary antibody
Anti-goat IgG	FITC	1:50	Donkey	n.a.	Abcam	Secondary antibody
CD16/CD32	Purified	1:50	Rat	2.4G2	BD Pharmingen	Fc block, binds to receptors for IgG
Western blot						
STAT3	Purified	1:3000	Mouse	84/Stat3	BD Transduction	Transcription factor
STAT5	Purified	1:500	Mouse	89/Stat5	BD Transduction	Transcription factor
β-actin	Purified	1:20,000	Mouse	AC-15	Sigma-Aldrich	
Anti-rabbit IgG	HRP	1:2000	Swine	polyclonal	Dako Cytomation	Secondary antibody
Anti-mouse IgG	HRP	1:2000	Rabbit	polyclonal	Dako Cytomation	Secondary antibody
Immunohistochemistry						
α-syn (Ab138501)	Purified	1:4000	Rabbit	n.s.m.	Abcam	Residues 118-123
CD11b	Purified	1:200	Rat	M1/70.15	AbD Serotec	See Flow Cytometry
CD4	Purified	1:200	Rat	GK1.5	AbD Serotec	See Flow Cytometry

(*Continued*)

http://dx.doi.org/10.1016/j.heliyon.2018.e00513

Table 1. (*Continued*)

Antibody	Coupled to	Dilution	Made in	Clone	Manufacturer	Function
Anti-mouse IgG	Biotin	1:2000	Horse	Polyclonal	Vector Laboratories	Recognized antibodies of mouse origin
Anti-rat IgG	Biotin	1:200	Goat	Polyclonal	Vector Laboratories	Secondary antibody
Anti-rabbit IgG	Biotin	1:200	Donkey	Polyclonal	Vector Laboratories	Secondary antibody
ELISA						
human-α-syn	Purified	1:1000–128.000	Mouse	4B12	Covance	For standard curve
-Anti-mouse IgG	HRP	1:2000	Rabbit	Polyclonal	DAKO	

n.s.m. Not supplied by the manufacturer; n.a. Not applicable.

BD Bioscience, Temse, Belgium; Dako Cytomation, Glostrup, Denmark; Aviva Biology Systems, San Diego, CA, USA; BioLegend, San Diego, CA, USA; eBioscience, San Diego, CA, USA; Abcam, Cambridge, United Kingdom; Vector Laboratories, Burlingame, CA, USA; AbD Serotec, Munich, Germany; Sigma-Aldrich, St. Louis, MO, USA; Pierce Antibodies, Rockford, IL, USA.

http://dx.doi.org/10.1016/j.heliyon.2018.e00513

doublets were removed by plotting FSC-H *vs.* FSC-A, and either 5000 CD3+CD4 +RFP+ Treg cells or 10,000 CD11b+ gated cells were acquired for analysis. The gates of positive CCR6, CD103, CD25, CD127, DR-D2, and DR-D3 cells were determined by the use of FMO (Fluorescence Minus One) for each of these antibodies.

2.6. Immunohistochemistry

Mice (n = 2 per group) were deeply anaesthetized with an overdose of pentobarbital and upon respiratory arrest perfused through the ascending aorta with ice-cold saline solution (without heparin) followed by 4% paraformaldehyde. The brains were post-fixed in paraformaldehyde for 4 h and left for cryoprotection in a 25% sucrose solution, thereafter sliced into 40 μm-thick coronal sections and separated into 4 full brain series. Immunohistochemistry was performed as before (Sanchez-Guajardo et al., 2010) on a full series for α-syn, and in one third of a series for CD11b, anti-mouse IgG, and CD4. Slides stained for α-syn were counter-stained with cresyl violet prior to cover slipping. Visualization was done using 3,3-diaminobenzidine and 0.1% of hydrogen peroxide for α-syn visualization, and 0.01% for the others. The sections were mounted on chrome-alum-coated glass slides and coverslipped. All antibodies are routinely tested for antigen specificity and titrated for adequate working dilution (for antibodies used, see Table 1).

Sections were analyzed by an observer blind to the identity of the samples on a Zeiss LSM710 microscope. For CD11b immunohistochemistry, representative coronal sections (3 for striatum and 2 for substantia nigra and hippocampus) from each animal were analyzed; both left and right hemispheres were counted separately. The sections selected distant from bregma were: −(2.8–3.3) mm for substantia nigra, −(1.58–2.0) for hippocampus, and +0.62–(−0.3) for striatum. A low power objective lens (1.25×, SPlan) was used to delineate the regions of interest (ROI) following anatomical points according to the mouse brain atlas (K. Franklin and G. Paxinos, The Mouse Brain in Stereotaxic Coordinates, Academic Press, San Diego, 1997). A fraction of the ROI (average of 16% for substantia nigra, 4.9% for striatum, and 9% for hippocampus) was sampled by using a counting frame placed randomly with the help of an automated software (VisioPharm Integrator Software, Hørsholm, Denmark), as to count between 40–50 CD11b+ cells per side and region using a 63× lens. While counting, microglia were profiled according to their morphology as previously described (Sanchez-Guajardo et al., 2010). Thereafter and based on the % of the ROI sampled (16% for substantia nigra, 4.9% for striatum, and 9% for hippocampus) we calculated the estimated number of cells in the total ROI (Total cell number estimated in area = (100% × number of cells counted)/% of ROI sampled) and calculated the ratio between Type A and Type B per animal. Each hemisphere was counted as duplicate and then average to obtained the number in the section,

http://dx.doi.org/10.1016/j.heliyon.2018.e00513

thereafter all sections counted per area (3 or 2 as mentioned above) were averaged, to obtain number of cells per brain area in each animal and the average and SD calculated per group when relevant; no stats were applied to this experiment due to the low number of animals.

CD4+ cells in brain were counted in equally distant (480 μm) coronal sections throughout the brain from prefrontal cortex until the beginning of cerebellum representing a third of a full series. The data is given as total number of CD4+ cells counted per animal. The analysis of α-syn was done on a full brain series and of IgG on a third of a full brain series.

2.7. SDS-PAGE and Western blot

Prior to SDS-PAGE and Western Blot analyses, the concentration of protein in the samples was determined using a bicinchoninic acid assay with a bovine serum albumin standard curve. A volume of cell lysate corresponding to 80 μg was transferred to an Eppendorf tube, and protein was precipitated by adding 9× volume of ice-cold 96% ethanol and left at −20 °C overnight. Next, tubes were centrifuged 20 min at 16,000 (4 °C) and the supernatant was carefully removed. Excess ethanol was allowed to evaporate for 10 min at 4 °C before the protein pellet was resuspended in 15 μl PBS. The protein solution was mixed with an SDS- and DTE-containing loading buffer prior to boiling and loading on an 8% Bis-Tris gel (VE vertical electrophoresis system, Hoefer, Holliston, MA, USA). After separation, proteins were blotted onto ethanol pre-activated polyvinylidene fluoride membrane membranes (GE Healthcare, Uppsala, Sweden) for 1.5 h in an ethanol-containing buffer using the Hoefer system. Thereafter, membranes were blocked with 5% skim milk in Tris-buffered saline with 0.05% Tween-20 (TBS-T) for 1 h at room temperature and then incubated with a primary antibody (Table 1) in 1% skim milk TBS-T solution overnight at 4 °C. On the following day, the membranes were washed 3 timed for 5 min each with TBS-T and incubated with the appropriate horseradish peroxidase (HRP)-conjugated secondary antibody (Table 1) in 1% milk in TBS-tween for 2 h at room temperature. The blots were visualized by enhanced chemiluminiscence (Amersham ECL Western Blotting detection reagents, GE Healthcare, Uppsala, Sweden) using a Fuji LAS-4000 ImageReader. Subsequently, blots were stripped for 30 min at 50 °C and incubated with a different primary antibody. The intensities of the protein bands were quantified using MultiGauge software and normalized to the level of β-actin in the sample. Full, non-adjusted western blots can bee seen in Supplementary Fig. 1.

2.8. Anti–α-syn antibody titration by ELISA

Prior to perfusion, retro-orbital blood samples were taken and allowed to coagulate for 24–48 h at 4 °C and centrifuged for 10 min at 400*g*. Serum was isolated and

http://dx.doi.org/10.1016/j.heliyon.2018.e00513

stored at −20 °C until analysis. The serum titer of anti-α-syn antibodies was analyzed by indirect ELISA. MaxiSorp 96-well ELISA plates (Thermo Fisher Scientific, Carlsbad, CA, USA) were coated overnight at 4 °C with 200 ng/well recombinant human α-syn (the same used to immunize the animals) in 100 mM carbonate/bicarbonate buffer, pH 9.6. After three washing steps using PBS with 0.05% Tween-20 (PBS-T), wells were blocked for two hours with 150 μl 0.2% bovine serum albumin in PBS-T, referred to as "blocking buffer". Next, 100 μl of serum samples serially diluted in blocking buffer were added for overnight incubation at 4 °C. Additionally, a standard curve to determine IgG concentration was generated from a 1 μg/μl monoclonal mouse anti-human α-syn IgG (dilution range 1:1000–1:128,000). All dilutions were run in duplicates. After rinsing in PBS-T, wells were incubated for two hours at room temperature with 100 μl HRP-conjugated monoclonal rabbit anti-mouse IgG in blocking buffer. As negative controls, either standard antibody or secondary antibody was omitted during incubations. Following three washes in PBS-T, plates were allowed to develop for 20–25 min with 100 μl 1-Step Ultra TMB-ELISA Substrate (Thermo Fisher Scientific, Carlsbad, CA) and reaction stopped by addition of 100 μl ready-to-use sulphuric acid Stop Solution (Thermo Fisher Scientific, Carlsbad, CA). Absorbance at 450 nm was read on a VersaMax plate reader (Molecular Devices, Sunnyvale, CA, USA). A log decay curve was fitted within the linear range of the standard curve (dilution range 1:48,000–1:2000 corresponding to 20.8×10^{-6} to 500×10^{-6} μg/μl standard antibody). The equation from the standard curve fit was used to calculate the concentration of anti-α-syn IgG (μg/μl) in the serum samples. All serum samples were diluted 400-fold before incubation, except those from animals having received fibrillar α-syn, for which 3200-fold dilution was used.

2.9. Statistical analysis

Statistical comparison of data was performed using Prism 6 software (GraphPad Software, La Jolla, CA, USA). Outliers where removed using the ROUT tests (q = 1). A parametric, one-way ANOVA assuming no matching/pairing of data and equal SD was done for all studies. When significant, it was followed by multiple comparisons of the means against each other with a Tukey test to determine significant changes between groups. Significance was accepted at the 95% probability level.

3. Results

With the aim to understand how and if the peripheral immune system, in particular the CD4 T cell pool, responded to increased local levels of the autologous protein α-syn, we inoculated Foxp3-RFP reporter mice with 100 μg of the recombinant wild-type human protein (monomeric) or its pathology-associated variants, nitrated α-syn and fibrillar α-syn. Naïve and LPS inoculated animals were used as a control (please refer to M&M).

http://dx.doi.org/10.1016/j.heliyon.2018.e00513

3.1. α-syn induces different reactions depending on its variant

Lymph node cells were isolated and the number of CD3+CD4+ and CD3+CD4− cells was determined by flow cytometry (Fig. 1A) that was reproducible in two independent experiments (n = 4 in each) (Fig. 2B). Nitrated α-syn increased the total number of T cells (CD3+), as both CD3+CD4+ cells (compared to all groups) and CD3+CD4− (compared to the other α-syn variants) were expanded (Fig. 2C–D). Monomeric and fibrillar α-syn did not induce T cell proliferation; however, monomeric α-syn significantly decreased the CD4+/CD4- ratio by reducing the CD4+ fraction in the T cell pool ($p = 0.0421$, Fig. 2E). Fibrillar α-syn significantly increased the percentage of CD3+CD4+Foxp3+ Tregs (Fig. 2B+F). Thus, the peripheral immune system can sense the variant of α-syn.

3.2. α-syn variants reduce the survival/activation capacities of Th cells and activate Treg

IL-2 is essential for survival of Treg and newly activated helper CD4 T cells, thus the IL-2 receptor α chain (CD25) is considered a marker of newly activated CD4 T cells (Waters et al., 2003). Flow cytometry analysis of CD25 expression (Fig. 3A) showed that increased levels of α-syn reduced the percentage of CD25+ helper T cells (CD3+CD4+Foxp3−, Th) irrespective of the variant, indicating that α-syn does not induce productive T cell activation (Fig. 3B). Additionally, fibrillar α-syn greatly reduced the expression of CD25 on Treg, which could compromise their survival and/or indicate that a new reservoir of resting Treg was generated in the periphery (Fig. 3C).

An important cytokine for naïve and memory T cell survival is IL-7, and thus its receptor α chain (CD127) is a marker for these T cells populations. Variants of α-syn appeared to also compromise the survival capacity of naïve/memory CD4 T cells in a variant-specific manner, as determined by flow cytometry (Fig. 3D), where fibrillar α-syn decreased CD127 on Th (Fig. 3E) and the monomeric form on Treg (Fig. 3F). Furthermore, the distribution between naïve/activated/memory Treg, as revealed by CCR6 and CD127 expression levels (Fig. 3G), was altered by α-syn variants (Table 2). All α-syn variants decreased the percentage of memory Treg (CCR6+CD127$^{lo/neg}$), as compared to the naïve animals, while nitrated and fibrillar α-syn increased the activated fraction (CCR6−CD127^{hi}) while contracting the naïve Treg compartment.

3.3. Variants of α-syn reduce STAT3 and fibrils induce α-syn antibody production

The titer of anti-monomeric α-syn antibody (IgG) was determined in serum, where we only observed a significant IgG production upon challenge with fibrillar α-syn (Fig. 4A–B). To determine the effect of locally increasing α-syn on the CD4 T cell

http://dx.doi.org/10.1016/j.heliyon.2018.e00513

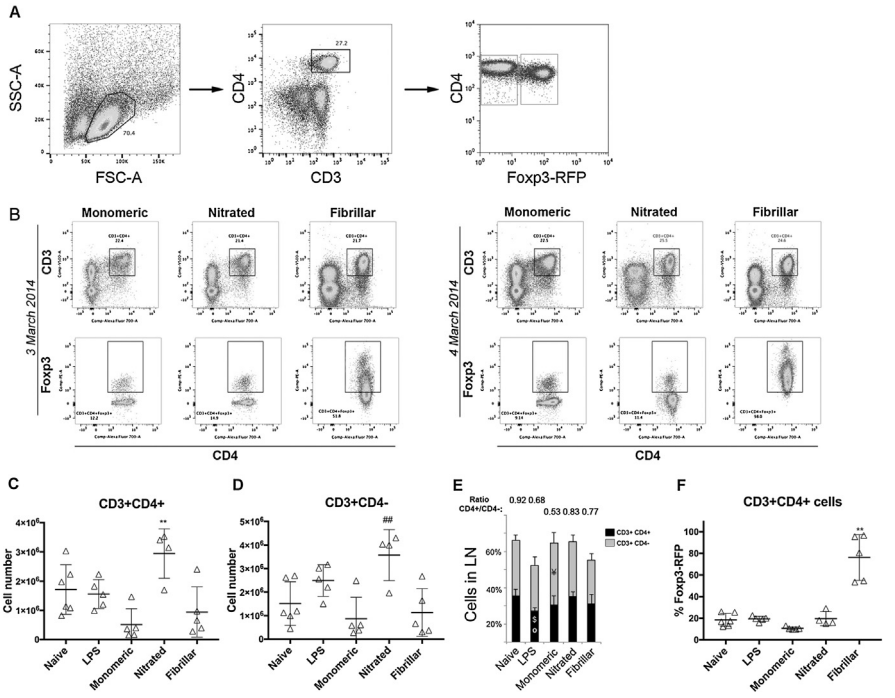

Fig. 2. T cell numbers in lymph nodes. Lymph node cells were analyzed by flow cytometry. A. Representative dot plot of the size *vs.* granularity of our sample which enabled us to gate live cells as it is well established the size and granularity of lymphocytes, and thus one can discard those too big, too small or with granules. The events within this gate where then plotted for CD3 and CD4 expression, those double positive (CD3+CD4+, upper right gate) are CD4+ T cells and those CD3+CD4− are assumed CD8+ T cells, as CD3 (TCR co-receptor) is only expressed in T lymphocytes. The CD3+CD4 + gated fraction was further plotted for CD4 *vs.* Foxp3+, and CD4+Foxp4+ gated to determine the percentage of regulatory T cells in our sample (Treg, upper-right gate). The percentage of effector cells was determined by gating on the CD4+Foxp3− population (Th, lower-right gate). The percentage given in each gate, represent the number of cells positive for a given combination of markers within the parent population, that is, the previous gate. B. Representative dot plots from two independent experiments showing CD4+Foxp3+ gated cells. C. Total number of CD3+CD4+ and D. Total number of CD3 +CD4− cells (grey). E. Percentage of CD4+ (black) and CD4− cells (grey) in lymph nodes. F. Percentage of CD3+CD4+Foxp3+ cells within the total CD3+CD4+ cell population. Average ± SD shown as a grey bar in C–E. One-way ANOVA followed by Tukey HSD, $p < 0.05$. * Different from all; # different from the other α-syn variants; ° different from naïve; $ different from nitrated; ¥ different from fibrillar. All numbers in the bar graphs are average + SD (3–4 independent experiments were conducted with n = 2–3 per group, after which all data was pooled to obtain a total n = 8–10 per group).

effector phenotype, we quantified the levels of STAT3 (its phosphorylation regulates the Th17/Treg balance) and STAT5 (downstream transcription factor of IL-2 (CD25 = IL-2Ra) and IL-7 (CD127 = IL-7Ra)) by western blot (Fig. 4C). All α-syn variants significantly reduced the level of expression of STAT3 (Fig. 4D). Despite the decrease in CD25, we did not observe any significant changes in its downstream transcription factor STAT5 (Fig. 4E). Our data for STAT expression shows a high variability, and this is also observed in some of the cytometry data; this is most likely be due to the fact that we pooled together the draining lymph nodes

http://dx.doi.org/10.1016/j.heliyon.2018.e00513

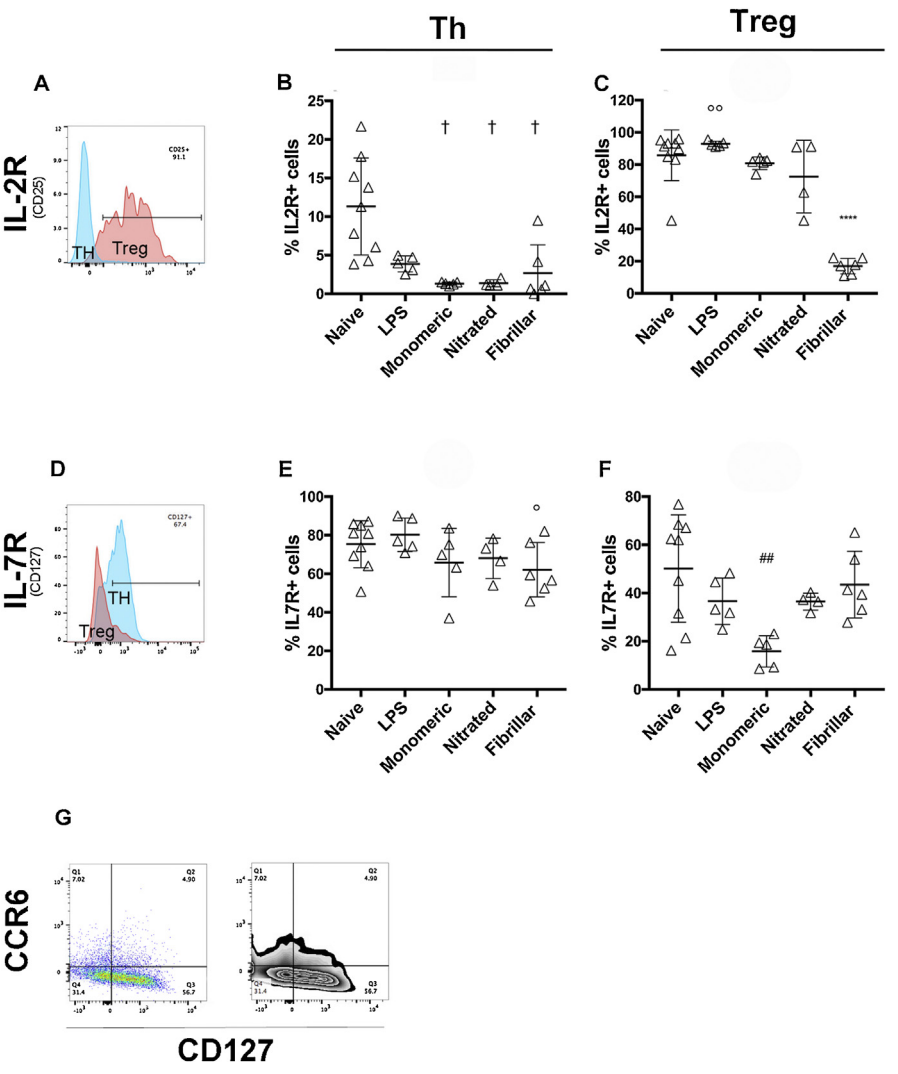

Fig. 3. IL-2Rα (CD25) and IL-7Rα (CD127) expression on CD3+CD4+ lymph node cells. Cells were gated for CD3+CD4+Foxp3− (*i.e.* Th) and CD3+CD4+Foxp3+ (*i.e.* Treg) as in Fig. 1. The gated events for Th and Treg where then plotted in a histogram to determine the percentage and level of expression of IL-2Rα (CD25) and IL-7Rα (CD127) in each population. Lack of CD25 or CD127 expression was determined by gating for the same population in a sampled where the antibody against CD25 or CD127 was omitted (FMO, not shown). All signal above this threshold is considered positive, and is gated to determine the percentage of CD25+ or CD127+ cells within the parent population (*i.e.* CD3+CD4+Foxp3+CD25+). Representative histograms showing the level of expression of IL-2Rα (A) and IL-7Rα (D) in Th (blue) and Treg (red) T cell populations. Graphs showing the average of cells expressing IL-2Rα (B & C) or IL-7Rα (E & F); grey bar is the average value ± SD. B & E are CD3+CD4+Foxp3− cells and C & F are CD3+CD4+Foxp3+ cells. G Representative dot plots of CD3+CD4+Foxp3+ cells expressing CD127 and CCR6. On the left, a semicolor dot plot that the allow us to see how many events are present, and on the right zebra dot plot to see where the boundaries of the different populations are. One-way ANOVA followed by Tukey HSD, $p < 0.05$. * Different from all; # different from the other α-syn variants; ° different from naïve; † different from LPS; § different from monomeric (3–4 independent experiments were conducted (n = 2–3 per group), after which all data was pooled to obtain a total n = 8–10 per group).

http://dx.doi.org/10.1016/j.heliyon.2018.e00513

Table 2. Activation state of Treg.

	Naïve	Activated	Memory	
	CCR6−CD127$^{lo/neg}$	CCR6−CD127^{hi}	CCR6+CD127$^{lo/neg}$	CCR6+CD127^{hi}
Naïve	54.4 ± 4.4	20 ± 9.5	13.8 ± 6.8	11.8 ± 3.9
LPS	66.6 ± 8.3	26.4 ± 9.2	4.6 ± 3.1°°	2.3 ± 1.2
Monomeric	62.9 ± 9.9	27.4 ± 6.8	5.8 ± 2.0°	3.9 ± 1.1
Nitrated	47.6 ± 4.9††	44.2 ± 6.8°°	4.1 ± 6.8°°	4.1 ± 1.7
Fibrillar	37.9 ± 7.8°°††§§	58.8 ± 9.2°°††§§	2.3 ± 1.0°°	1.0 ± 0.8

Values were obtained by means of flow cytometry, Treg cells are CD3+CD4+Foxp3+.
Values presented are averages ± SD.
3–4 independent experiments were conducted (n = 2–3 per group).
All data was pooled to obtain a total n = 8–10 per group.
°Different from naïve; † different from LPS; § different from monomeric.
One symbol $p \leq 0.05$; two symbols $p \leq 0.01$.
One-way ANOVA followed by Tukey HSD, $p < 0.05$.

adjacent to the injection site (inguinal) and the axillar and braquial ones, which will varyingly react to an event happening at another site. Additionally, the STAT data was obtained from an homogenate of all lymph node cells, which means the results are diluted by cells other than CD4 T cells (CD8 T cells and B cells mainly).

3.4. Monomeric and nitrated α-syn modulate dopamine receptor expression

Dopamine is known to be a contributing factor in lymphocyte regulation, and at the same time dopamine can form complexes with α-syn and increase its oligomerization (Cappai et al., 2005; Conway et al., 2001; Lee et al., 2011; Outeiro et al., 2009). By flow cytometry, we analyzed two DRs (Fig. 5A) known to have opposite effects on CD4 T cells: DR-D2, associated with T cell regulatory functions, and DR-D3, which is suggested to induce pro-inflammatory responses and has been implicated in the detrimental T cell response in the MPTP model of PD (Gonzalez et al., 2013; Tinsley et al., 2009). In the naïve animal, as in all other conditions, at least 30% of Th cells do not express DRs (Fig. 5B). DR-D3 was significantly increased by nitrated α-syn (Fig. 5D & H), although a similar trend was also observed in the LPS group. DR-D2 expression was decreased by the nitrated form in Treg (Fig. 5G) and by monomeric α-syn both in Th (Fig. 5C) and Treg (Fig. 5G) cells. Fibrillar α-syn, however, did not induce modulation of these DRs (Fig. 5B–I). As a note, while the double positive DR-D2+D3+ fraction in Th was significantly reduced by monomeric α-syn (Fig. 5E), this variant induced a concomitant increase of this population in the Treg fraction (Fig. 5I).

http://dx.doi.org/10.1016/j.heliyon.2018.e00513

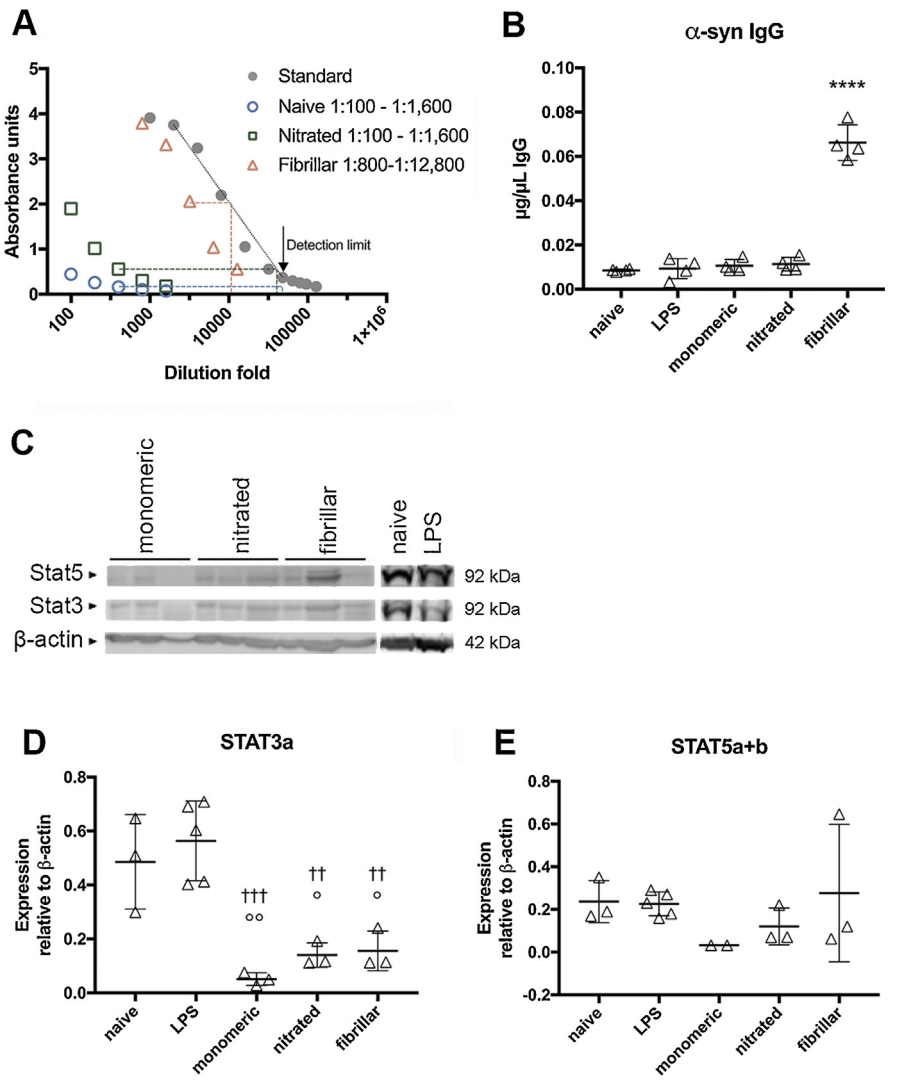

Fig. 4. T cell differentiation. A: Actual ELISA data depicted to demonstrate calculation of serum anti-α-syn IgG concentration from absorbance. Standard curve (grey filled circles) is shown diluted from 1:1000 to 1:128;000. The linear range is indicated by a dashed line (dilution 1:2000 to 1:48,000). Color symbols show dilution series from experimental groups, and colored dashed lines indicate the conversion from absorbance to the corresponding antibody concentration. Functional detection limit is indicated (black arrow). Note that samples from animals inoculated with fibrillar α-syn were used at 1:3200 dilution instead of 1:400 due to higher antibody concentration. B Graph showing the average ± SD concentration of anti-α-syn antibodies in serum (μg/μl). All samples were done in duplicates (n = 4/group). C Lymph nodes cells were incubated *in vitro* for 6 h without activation and thereafter lysed for analysis by SDS-PAGE. Representative blots for each protein studied. Band intensity was quantified and normalized to the intensity of β-actin. D–E Graphs showing the average relative value ± SD of normalized levels of protein in lymph node cell lysates (n = 3–5 samples/group). One-way ANOVA followed by Tukey HSD, $p < 0.05$. * Different from all; ° different from naïve; † different from LPS.

http://dx.doi.org/10.1016/j.heliyon.2018.e00513

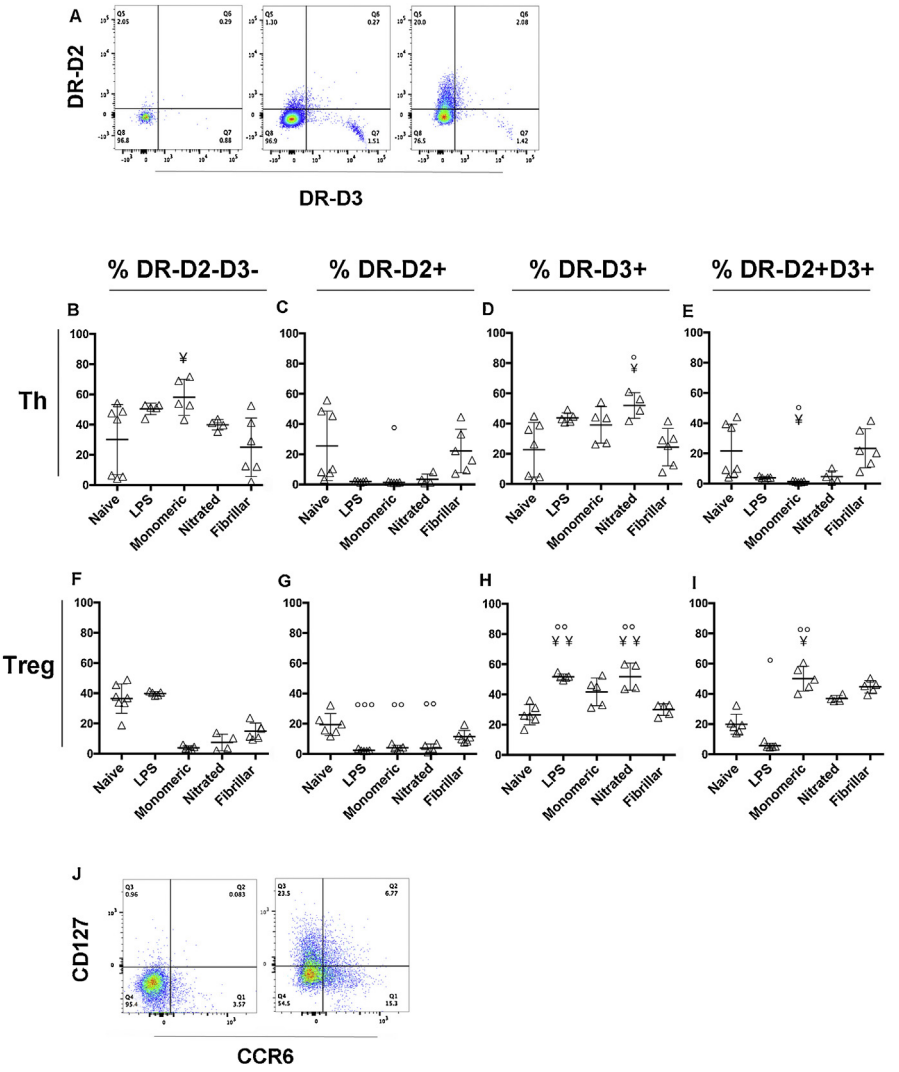

Fig. 5. Dopamine receptor D2 and D3 expression on CD3+CD4+ cells. Th and Treg were gated as before, and the percentage of cells positive for dopamine receptor DR-D2 and DR-D3 were determined. A Representative dot plots for a sample with no staining for DR (FM-DR-D2 and DR-D3, left plot) and for two samples co-stained for DR-D2 and DR-D3 (center and right plots). The relative percentages of the different populations are shown as scatter graphs: Double negative (DR−D2−D3−; B & F), DR−D2+ (C & G), DR−D3+ (D & H) and double positive (DR−D2+D3+; E & I) cells within the Th (B–E) and Treg (F–I). The average value is shown as a grey bar ± SD. J. Representative dot plots showing CD3+CD4+Foxp3+ cells gated for DRs. Left dot-plot, a sample with no staining for CCR6 and CD103 (FM-CCR6 and CD103), right dot plot a sample co-stained for CCR6 and CD103. One-way ANOVA followed by Tukey HSD, $p < 0.05$. ° Different from naïve; ¥ different from fibrillar (3–4 independent experiments were conducted (n = 2–3 per group), after which all data was pooled to obtain a total n = 8–10 per group).

http://dx.doi.org/10.1016/j.heliyon.2018.e00513

3.5. CD4 T cell homing (CCR6) and tolerance (CD103) capacity is modulated by α-syn

To determine whether the increase of α-syn had modified the capability of T cells to migrate to the brain, we measured the expression of CCR6, a chemokine receptor implicated in T cell brain homing in the experimental autoimmune encephalomyelitis (EAE) animal model of multiple sclerosis (Reboldi et al., 2009). We also studied the expression of CD103, a lectin involved in cell-cell induced tolerance and T cell extravasation (Fig. 5J) (Huang et al., 2013). The fraction of CCR6+ cells within the total Th pool was approximately 10%, and this was significantly reduced upon challenging of the periphery with α-syn (Table 2). About 30% of the Treg fraction expressed CCR6, and its expression was only significantly reduced by fibrillar α-syn (Table 3). Almost no Th or Treg cells expressed CD103. Furthermore, we observed that all the cells expressing CD103 and CCR6 were also single DR+ (Tables 4 and 5), only a very small fraction of DR-negative Tregs expressed them (Table 4), never the DR−D2+D3+.

Table 3. Percentage of CD4 T cells expressing CCR6 and CD103.

	Th (CD3+CD4+Foxp3−)			
	CCR6+	**CCR6+CD103+**	**CD103+**	**CCR6−CD103−**
Naïve	7.8 ± 7.1	0.2 ± 0.1	0.2 ± 0.2	91.8 ± 7.0
LPS	2.1 ± 0.5°	0.1 ± 0.1	0.2 ± 0.2	97.6 ± 0.7°
Monomeric	2.4 ± 0.9	0.0 ± 0.0	0.1 ± 0.0	97.5 ± 0.9°
Nitrated	1.6 ± 1.0°	0.1 ± 0.0	0.2 ± 0.0	98.1 ± 1.1°
Fibrillar	1.3 ± 1.0°	0.0 ± 0.0	0.1 ± 0.1	98.5 ± 1.0°
	Treg (CD3+CD4+Foxp3+)			
	CCR6+	**CCR6+CD103+**	**CD103+**	**CCR6−CD103−**
Naïve	28.4 ± 18.4	1.2 ± 0.2	2.7 ± 2.9	67.6 ± 16.0
LPS	18.0 ± 5.9	0.7 ± 7	1.6 ± 1.4	80.0 ± 7.9
Monomeric	21.0 ± 2.3	0.6 ± 0.3	1.2 ± 0.6	77.2 ± 2.9
Nitrated	17.0 ± 8.6	1.9 ± 0.7††	2.8 ± 1.0##	78.2 ± 8.9
Fibrillar	8.5 ± 3.5°°	0.1 ± 0.1	0.2 ± 0.2	91.2 ± 3.7°°

Values were obtained by means of flow cytometry.
Values presented are average percent ± SD.
3–4 independent experiments were conducted (n = 2–3 per group).
Data was pooled to obtain a total n = 8–10 per group.
°Different from naïve; † different from LPS; # different from the other α-syn.
One symbol $p \leq 0.05$; two symbols $p \leq 0.01$.
One-way ANOVA followed by Tukey HSD, $p < 0.05$.

http://dx.doi.org/10.1016/j.heliyon.2018.e00513

Table 4. Th expression of CCR6 and CD103 as a function of DR expression.

	DR−D2+			
	CCR6+	**CCR6+CD103+**	**CD103+**	**CCR6−CD103−**
Naïve	8.6 ± 7.11	3.8 ± 3.2	10.4 ± 3.5	78.2 ± 13.1
LPS	13.5 ± 0.6●●	16.5 ± 4.3**	10.6 ± 1.9	59.4 ± 6.0
Monomeric	5.7 ± 1.5	8.7 ± 5.3¥¥	39.5 ± 5.1**	44.1 ± 7.6°°##
Nitrated	2.6 ± 1.4	1.9 ± 0.9	27.3 ± 5.1**	85.65 ± 16.1
Fibrillar	12.3 ± 2.0	4.3 ± 0.4	44.8 ± 3.7##	30.1 ± 4.3††
	DR−D3+			
	CCR6+	**CCR6+CD103+**	**CD103+**	**CCR6−CD103−**
Naïve	3.1 ± 2.7	2.9 ± 2.8	21.3 ± 16.7	72.6 ± 21.8
LPS	4.0 ± 0.5●●	2.5 ± 0.8	11.4 ± 0.8	82.0 ± 1.3
Monomeric	0.8 ± 0.4	1.3 ± 0.7	39.8 ± 7.2¥¥††	58.0 ± 8.3¥
Nitrated	0.6 ± 0.5	0.7 ± 0.5	27.8 ± 9.1	71.0 ± 16.1
Fibrillar	0.5 ± 0.5	0.6 ± 0.7	13.7 ± 5.7	85.3 ± 6.0

Values were obtained by means of flow cytometry, Th cells are CD3+CD4+.
Values presented are average percent ± SD.
3–4 independent experiments were conducted (n = 2–3 per group).
Data was pooled to obtain a total n = 8–10 per group.
°Different from naïve; † different from LPS; # different from the other α-syn; *different from all; ¥ different from fibrillar α-syn; ● different from all α-syn variants.
One symbol $p \leq 0.05$; two symbols $p \leq 0.01$.
One-way ANOVA followed by Tukey HSD, $p < 0.05$.

In the Th pool (Table 4), all α-syn variants increased the expression of CD103 on DR−D2+ cells, while on DR−D3+ cells monomeric increased it, nitrated had no effect and fibrillar α-syn decreased it. α-syn variants did not seem to have any effect on CCR6 expression, which was only expressed on DR−D2+ cells.

On Treg cells (Table 5), α-syn variants regulated specifically the expression of CD103: Monomeric α-syn significantly increased CD103+ in the DR−D2+ and the DR−D3+ populations; nitrated the CCR6+CD103+ in the DR−D2+; and fibrillar α-syn increased CD103+ in the DR−D2+ cells while it decreased it in the DR−D3+ population. This suggests a link between dopamine signaling on CD4 T cells and CD103 expression.

3.6. Brain microglia are modulated as a result of increased α-syn variants in the periphery

In order to address whether peripheral immune response to α-syn injection could induce a response in brain microglia, we analyzed the expression of different

http://dx.doi.org/10.1016/j.heliyon.2018.e00513

Table 5. Treg expression of CCR6 and CD103 as a function of DR expression.

	DR−D2−DR−D3−			
	CCR6+	**CCR6+CD103+**	**CD103+**	**CCR6−CD103−**
Naïve	8.0 ± 6.1	0.8 ± 0.8	5.4 ± 3.7	86.1 ± 6.6
LPS	3.2 ± 1.4	0.4 ± 0.04	9.3 ± 5.0	87.2 ± 6.5
Monomeric	4.9 ± 1.7°°¥¥	0.3 ± 0.07	3.5 ± 1.3°	91.3 ± 3.2
Nitrated	3.9 ± 1.5	0.8 ± 0.2	7.1 ± 2.4	88.2 ± 3.1
Fibrillar	1.0 ± 1.0	0.1 ± 0.1	0.8 ± 1.1°°††	98.2 ± 2.1°†
	DR−D2+			
	CCR6+	**CCR6+CD103+**	**CD103+**	**CCR6−CD103−**
Naïve	10.8 ± 3.9	3.1 ± 1.8	12.7 ± 4.4	70.8 ± 5.9
LPS	31.3 ± 2.07**	12.1 ± 4.4°°	8.5 ± 4.7	46.1 ± 5.5
Monomeric	16.8 ± 4.6	17.6 ± 5.3°$	29.2 ± 16.2**	42.7 ± 10.9°°
Nitrated	10.5 ± 4.0	10.2 ± 5.3°	21.9 ± 9.7	57.4 ± 14.3°°
Fibrillar	15.9 ± 6.4	7.6 ± 6.4	31.8 ± 8.4##	44.6 ± 8.4**
	DR−D3+			
	CCR6+	**CCR6+CD103+**	**CD103+**	**CCR6−CD103−**
Naïve	11.7 ± 6.5	13.0 ± 10.3	26.1 ± 4.8	49.2 ± 21.1
LPS	28.0 ± 2.58●●	13.6 ± 4.2	18.5 ± 1.1	39.9 ± 6.7
Monomeric	9.3 ± 1.1	10.6 ± 3.3	35.4 ± 2.2†	44.9 ± 4.1
Nitrated	8.9 ± 4.1	8.7 ± 3.8	33.3 ± 15.2†	49.1 ± 14.9
Fibrillar	6.1 ± 4.0	0.9 ± .09	7.4 ± 4.9°°##	85.6 ± 8.7**

Values were obtained by means of flow cytometry, Treg cells are CD3+CD4+Foxp3+.
Values presented are averages ± SD.
3–4 independent experiments were conducted (n = 2–3 per group).
Data was pooled to obtain a total n = 8–10 per group.
°Different from naïve; † different from LPS; # different from the other α-syn; * different from all; ¥ different from fibrillar α-syn; $ different from nitrated α-syn; ● different from all α-syn variants.
One symbol $p \leq 0.05$; two symbols $p \leq 0.01$.
One-way ANOVA followed by Tukey HSD, $p < 0.05$.

markers by flow cytometry upon gating on CD11b+ cells (Fig. 6A). We observed changes in the markers related to tolerance (Fig. 6B) or T cell interactions (Fig. 6C). Monomeric α-syn induced an increase of several markers (CD154, CD103, and CD54), while nitrated α-syn reduced CD4 expression in microglia. Fibrillar α-syn both reduced (CD4 and CD11c) and increased (CD154 and CD103) microglial surface proteins. Thus, brain microglia reacted specifically to the α-syn variant that the peripheral immune system was challenged with. Interestingly, all variants increased CD200R, albeit with different potency (Fig. 6B).

http://dx.doi.org/10.1016/j.heliyon.2018.e00513

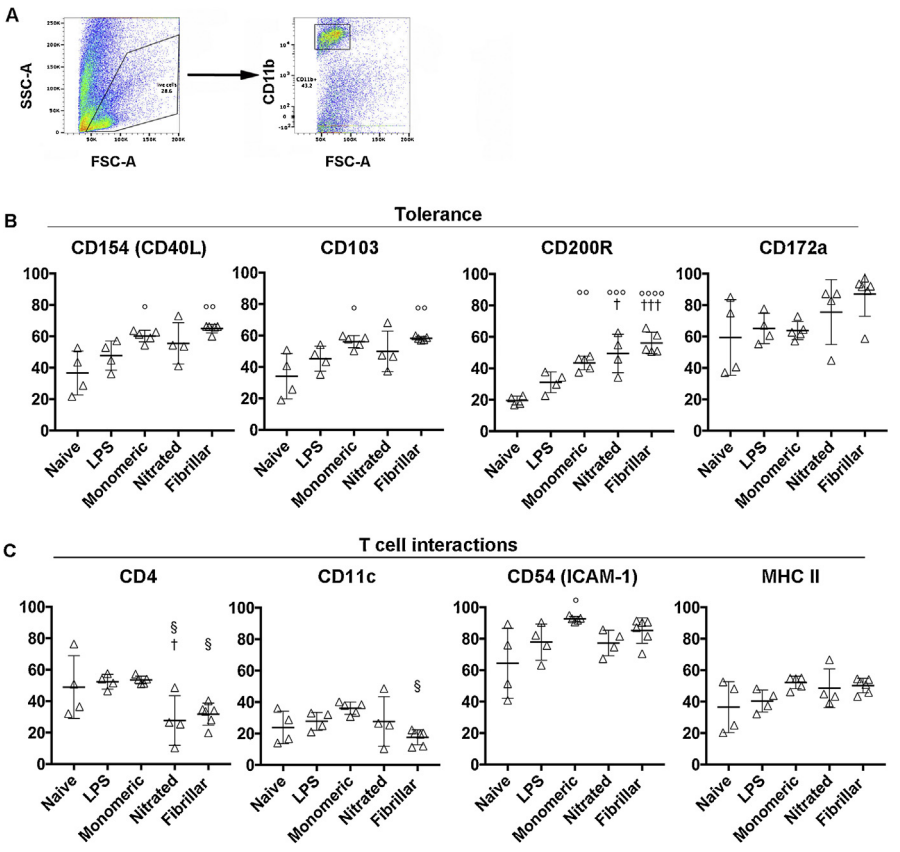

Fig. 6. Percentage of microglia expressing activation markers. (A) Representative dot plots showing the gating strategy for live CD11b+ cells. Bar graphs representing the average percentage + SD of microglia expressing activation markers related to tolerance (B) or adaptive immunity (C). One-way ANOVA followed by Tukey HSD, $p < 0.05$. ° Different from naïve; • different from all α-syn variants; † different from LPS; ¥ different from fibrillar α-syn (3–4 independent experiments were conducted (n = 2–3 per group), after which all data was pooled to obtain a total n = 8–10 per group).

Challenging the periphery with α-syn variants increased co-expression of markers as compared to naïve or LPS (Table 6), suggestive of a polarization of the microglia population. In particular, monomeric and fibrillar α-syn lead to co-expression of specific markers above 50–60% (Table 6A + C). Monomeric (Table 6A) induced co-expression of CD54 with CD4 and MHC-II, while CD4 showed 40% co-expression with MHCII. In the case of fibrils (Table 6C), CD172 was co-expressed with CD200R or with CD54. Thus, half of the microglia became CD4+CD54+MHC-II+ when monomeric α-syn was increased in the periphery, while it became either CD172+CD200R+ or CD4+CD172+MHC-II+ (CD4 & MHC-II co-express 49%) when challenged with fibrillar α-syn. Interestingly, nitrated α-syn (Table 6B) did not induce any particular polarization of microglia.

As a supplement to the cytometric analysis we performed histology in a small number of animals. CD11b immunostaining in representative sections throughout

http://dx.doi.org/10.1016/j.heliyon.2018.e00513

Table 6. Percentage of correlation between microglia's surface proteins expression.

A	***Monomeric α-syn***						
	CD103	**CD200R**	**CD54**	**CD11c**	**CD4**	**MHCII**	**CD154**
CD172a	11	37	33°°	9	33	43	26
CD103		21	48	16	44	12	43
CD200R			11	5	12	14	11
CD54				15	56††	***55***°	43
CD11C					27	8	37
CD4						40††¥	44
MHCII							38
B	***Nitrated α-syn***						
	CD103	**CD200R**	**CD54**	**CD11c**	**CD4**	**MHCII**	**CD154**
CD172a	24	46	44°	16	32	44	37
CD103		26	35	15	32	23	36
CD200R			24	12	24	25	24
CD54				15	39	45	34
CD11C					21	26	26
CD4						31	33
MHCII							36
C	***Fibrillar a-syn***						
	CD103	**CD200R**	**CD54**	**CD11c**	**CD4**	**MHCII**	**CD154**
CD172a	26	57††	61°	4	19	51	48
CD103		12	35	4	25	5	29
CD200R			16	1	9	11	13
CD54				4	37	49	34
CD11C					7	2	19
CD4						19	25
MHCII							28
D	***LPS***						
	CD103	**CD200R**	**CD54**	**CD11c**	**CD4**	**MHCII**	**CD154**
CD172a	7	25	36	12	27	17	14
CD103		4	7	4	3	7	6
CD200R			16	5	5	8	5
CD54				7	14	12°··	8
CD11C					4	10	4
CD4						9	6
MHCII							3

http://dx.doi.org/10.1016/j.heliyon.2018.e00513

C	*Naïve*						
	CD103	**CD200R**	**CD54**	**CD11c**	**CD4**	**MHCII**	**CD154**
CD172a	20	37	69	25	42	33	22
CD103		11	19	17	17	2	16
CD200R			34	16	15	25	11
CD54				23	25	35	17
CD11C					15	24	11
CD4						24	13
MHCII							2

Values were obtained by means of flow cytometry, Treg cells are CD3+CD4+Foxp3+.
Values presented are averages ± SD.
3–4 independent experiments were conducted (n = 2–3 per group).
All data was pooled to obtain a total n = 8–10 per group.
°Different from naïve; † different from LPS; ¥ different from fibrillar α-syn; ● different from all α-syn variants.
One symbol $p \leq 0.05$; two symbols $p \leq 0.01$.
One-way ANOVA followed by Tukey HSD, $p < 0.05$.

the brain did not show any overt microgliosis (drastic change in number or cell profile) in any brain area. We further analyzed CD11b+ microglia in representative sections of substantia nigra and striatum (for their relevance in PD) and hippocampus (due to its high constitutive α-syn expression) (Fig. 7). We have previously shown that rat and marmoset brains possess two main type of CD11b+ microglia profiles: resting/surveillant type A (small cell bodies with 2–3 thin ramifications and few secondary ones, arrows Fig. 7J & K) and the hyper-ramified type B (cells with numerous secondary and tertiary ramifications with sometimes a slightly bigger cytoplasm, arrowheads in Fig. 7) (Barkholt et al., 2012; Sanchez-Guajardo et al., 2010). One analyzed naïve mouse showed CD11b+ type A as the most abundant cell in striatum (ratio A:B 4.0) and substantia nigra (ratio A:B 3.3), as well as in in two animals injected peripherally with fibrillar α-syn (ratio A:B in striatum 2.5 ± 0.25; and in substantia nigra 2.4 ± 0.69) (arrows, Fig. 7G & H). However, the hyper-ramified type B microglia were more abundant in the mouse peripherally challenged with monomeric (ration A:B in substantia nigra 1.2 and striatum 1.3) (arrowheads in Fig. 7A & B) and in the two mice injected with nitrated α-syn (ratio A:B in substantia nigra 1.3 ± 0.65, and in striatum 1.0 ± 0.35, arrowheads in Fig. 7D & E) where they appeared in equal numbers as the resting/surveillant microglia (not shown for these groups), suggesting a response in the CD11b+ population. The morphological changes appear to be specific to the nigrostriatal pathway as they were not observed in hippocampus where the hyper-ramified type B microglia (Fig. 7C, F & I) appeared in a ratio 1:1 with the type A surveillant CD11b+. The higher number of type B in this region in all groups may

http://dx.doi.org/10.1016/j.heliyon.2018.e00513

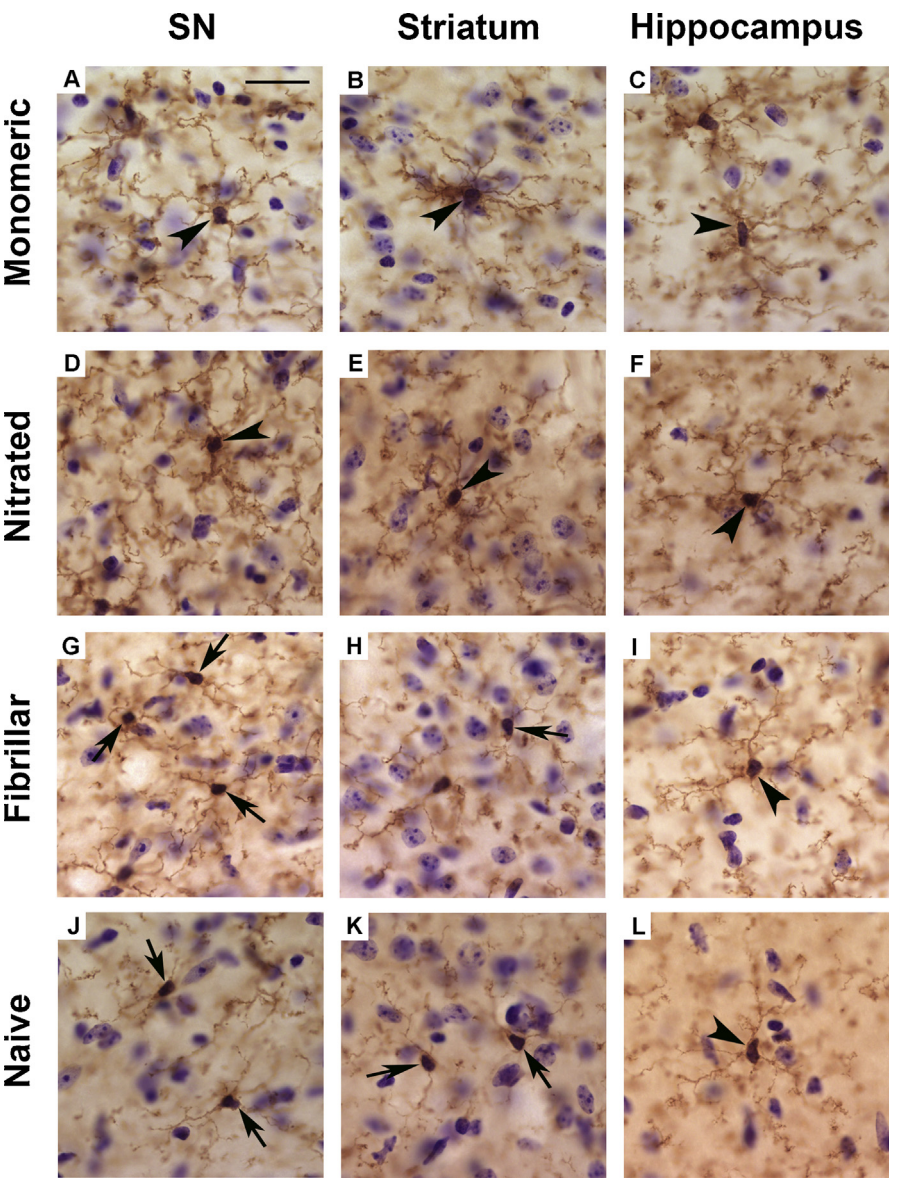

Fig. 7. CD11b immunopositive microglia in striatum, hippocampus, and substantia nigra. A series of coronal brain sections were immunostained with anti-CD11b antibody to assess changes in microglia cell number and/or morphology. Photos show representative images of microglia morphology in substantia nigra (A, D, G, J), striatum (B, E, H, K), and hippocampus (C, F, I, L) of animals having received monomeric α-syn (A-C), nitrated α-syn (D–F), or fibrillar α-syn (G–I), and from a naïve mouse (J–L). Two main types of microglia were found in brain: resting/surveillant type A microglia (small cell bodies with 2–3 thin ramifications and few secondary ones, arrows) and the hyper-ramified type B (cells with numerous secondary and tertiary ramifications that sometimes appeared thicker and often with bigger cytoplasm, arrowheads). Animals receiving nitrated or monomeric α-syn exhibited a greater number of hyper-ramified CD11b+ (type B, arrowheads) cells in substantia nigra (A & D) and striatum (B & E) than naïve animals, which showed mostly type A resting/surveillant microglia (arrows) (J & K). The animals receiving fibrillar α-syn showed type A as the main CD11b+ cell type (G & H). In hippocampus all animal showed Type B CD11b+ cells (arrow, C, F, I & L) as numerous as type A (not shown) Scale bar in A applies to all: 20 μm (n = 2, one experiment).

http://dx.doi.org/10.1016/j.heliyon.2018.e00513

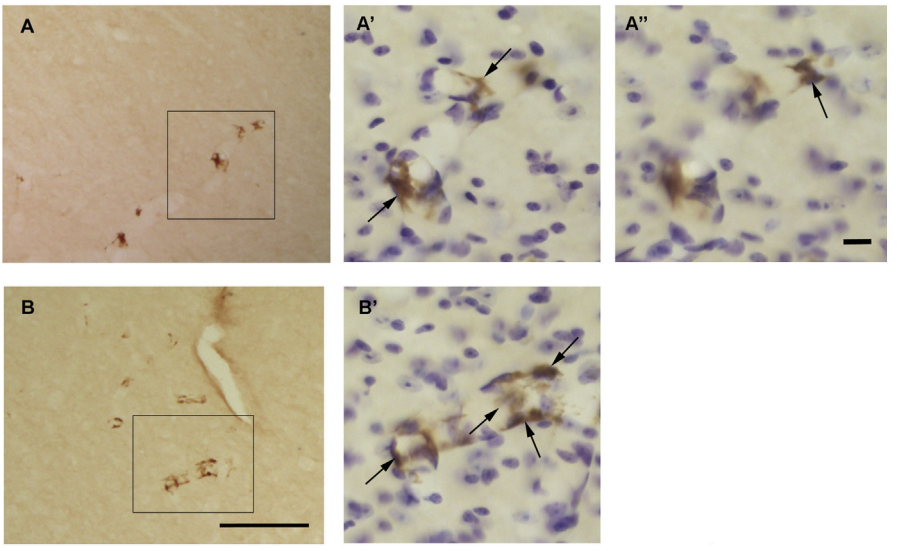

Fig. 8. α-syn brain immunostaining. Representative substantia nigra photomicrographs from two different monomeric α-syn animals stained for anti-human α-syn (A & B). A', A" and B' show magnification of blood vessels with α-syn+ cells co-stained with cresyl violet to see the cellular environment. Scale bar: B = 100 μm, and A" = 10 μm.

be related to the high plasticity known to happen (Grabert et al., 2016): naïve (Ratio A:B 1.0), monomeric (Ratio A:B 0.9), fibrillar (Ratio A:B 1.1 ± 0.38) and nitrated (Ratio A:B 0.7 ± 0.12). Note that due to the low number of animals used for sampling no statistical analysis was performed, and although we cannot draw conclusion from the histological data, they give weight to our cytometry data and suggest that microglia responded by changing their protein expression (cytometry) and their profile (histology) upon peripheral injections of α-syn in variant-dependent manner in some areas of the brains such as in the nigrostriatal system.

3.7. No deposition of α-syn in the brain

Representative coronal sections covering all the brain were immunostained with antibodies against human α-syn to assess any possible accumulation of the peripherally injected α-syn in brain parenchyma. We did not observe any positive staining throughout the brain in any of the groups five days after the second inoculation (data not shown). However, we did observe specifically in the group challenged with monomeric α-syn that blood vessels throughout the brain showed α-syn+ staining of small, ramified perivascular cells (Fig. 8).

3.8. Peripheral α-syn challenge results in CD4+ T cells and IgG + round cells migrating into brain parenchyma

A representative series of coronal sections throughout the brain were stained for CD4, and all positive cells in each section were counted. We observed that all α-syn variants induced infiltration of CD4+ round cells into parenchyma

http://dx.doi.org/10.1016/j.heliyon.2018.e00513

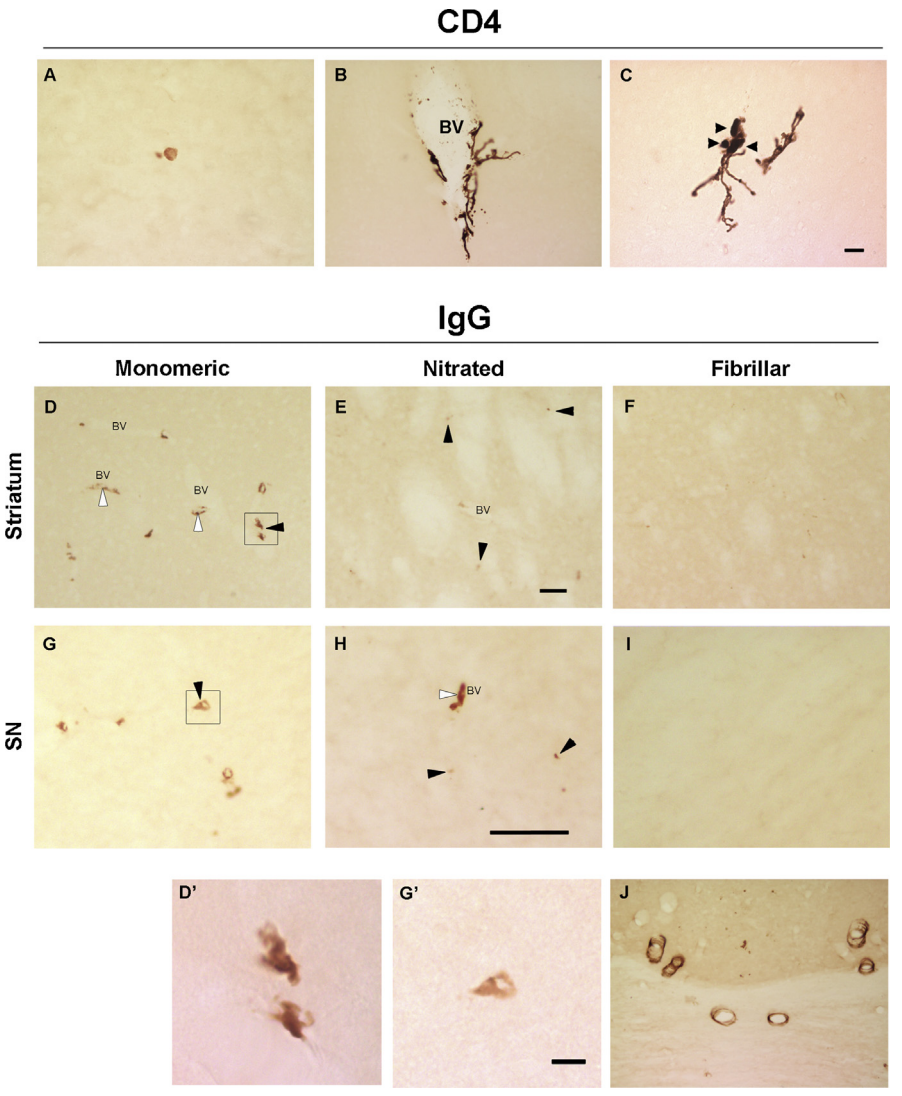

Fig. 9. CD4+ and IgG+ cells in brain parenchyma. Representative brain photomicrographs of a mouse inoculated with monomeric α-syn stained for CD4 (A–C). (A) A round CD4+ cell in parenchyma. (B) A CD4+ microglia-like cell in association with a blood vessel. (C) A CD4+ microglia-like cell in touch with small round CD4+ cells (arrowheads). Scale bar: 10 μm, applies to all. Representative photomicrographs of brain sections stained for mouse IgG (D–J): In striatum (D–F) and substantia nigra (SN, G–I), from mice receiving monomeric α-syn (D & G), nitrated α-syn (E & H), or fibrillar α-syn (F & I). BV, blood vessel; black arrowhead, positive cell in parenchyma; white arrowhead, positive cell in a blood vessel; squares are magnified in D' and G'. (D') Small, ramified IgG+ cells. (G') Small, round IgG+ cell. (J) Representative photomicrograph of a brain section from the monomeric α-syn group stained for mouse-IgG showing IgG+ blood vessels. Scale bar in (H) (100 μm) applies to (D–J); in (G') (10 μm) applies to (D' & G').

(monomeric 55–75, nitrated 22–42, fibrillar 78–108; Fig. 9A). These were isolated and distributed throughout the brain, not accumulating in any particular brain area. In our hands, and with this approach we usually only see between 2–5 CD4+ round cells throughout a naïve brain (data not shown). The monomeric and nitrated α-syn

http://dx.doi.org/10.1016/j.heliyon.2018.e00513

groups additionally showed CD4+ microglia-like cells associated with blood vessels (Fig. 9B), but only the nitrated group had CD4+ microglia-like cells in parenchyma which on occasions were seen in contact with CD4+ round non-ramified cells (Fig. 9C).

When adjacent brain sections were stained for mouse IgG, we observed IgG+ cells in striatum (Fig. 9D & E) and substantia nigra (Fig. 9G & H) from the monomeric and nitrated α-syn groups, but not in the fibrillar group (Fig. 9F & I). The IgG+ cells were either found luminal/associated to blood vessels (BV in Fig. 9D, H & E) or in parenchyma (Fig. 9D' & G'), and these had either an irregular cell body with ramifications (Fig. 9D'), or round morphology reminiscent of B cells (Fig. 9G'). Additionally, many blood vessels stained positive for IgG in the monomeric group throughout the brain (Fig. 9J).

4. Discussion

Great attention has been put into the effect of extracellular α-syn on microglia and neurons in PD, but little is known about the effect that α-syn has on the peripheral immune system. Here we analyzed the response of the immune system to a peripheral local increase in α-syn or its PD-associated pathogenic variants. We specifically focused on CD4+ lymphocytes, which have been highlighted as a key population during PD-like neurodegeneration (Brochard et al., 2009). To do so, we challenged naïve Foxp3-RFP mice with wild type human monomeric, nitrated or fibrillar α-syn (100 μg) in order to understand how changes in α-syn during PD may affect the peripheral CD4+ T cells. In parallel we included a group of animals inoculated with LPS (10,000 EU/g) to establish the specificity of the α-syn-induced changes as compared to the well-established pro-inflammatory response to LPS, which is known to induce immune activation not only in periphery but also in brain (Castano et al., 2002; Gao et al., 2011). A group of naïve animals was also included to determine the baseline of immunological parameters, allowing comparison to the homeostatic state. Importantly, our study was undertaken in absence of human α-syn expression, pathology or deposition in the brain, enabling us to dissect the effects induced by α-syn in the periphery from the ones induced as a result of pathological events in the brain. This also allowed us to study the impact of these peripheral immune events on brain microglia, shedding light on the crosstalk between peripheral immunity and brain immunity. In humans, α-syn increases in immune cells as we age, a process more accentuated in PD (Gardai et al., 2013; Kim et al., 2004; Shin et al., 2000). Here, we do not mimic this gradual increase, but rather an acute increase of local α-syn availability; thus, we can pinpoint the actual processes involved in the breakage of tolerance to α-syn and how this reaction varies as the protein is modified by aggregation or oxidation (*i.e.* pathology progression). This is crucial for dissecting the different ongoing processes during PD pathology, which are obscured and mingled during a constant gradual increase of α-syn and its

http://dx.doi.org/10.1016/j.heliyon.2018.e00513

pathological variants that overlap over time, thus making it difficult to understand how the peripheral immune system is affected during PD.

4.1. α-syn variants affect the survival capacities of CD4 T cells

Monomeric or fibrillar α-syn did not induce any significant change in the CD4 T cell numbers, suggesting suboptimal or lack of TCR-MHC-II contact with CD4 T cells, and thus an adaptive immune response was not triggered. On the other hand, nitrated α-syn increased number of CD4+ and CD4- cells, suggesting that while nitrated was considered non-self (pathogenic), monomeric and fibrillar were treated as self. However, the significant reduction in CD25 expression was a common finding for all α-syn variants, which indicates that the T cells expanding due to nitrated α-syn were probably not viable. CD4+ T cells in PD patients are reduced (Bas et al., 2001; Gruden et al., 2011; Stevens et al., 2012), a reduction reflected in the altered CD4:CD8 ratio observed (Baba et al., 2005; Bas et al., 2001; Hisanaga et al., 2001). It is still unclear though, if this net reduction is due to the contraction of the CD4 T cell compartment as whole or a change in the balance between its different activation stages. Our data regarding the decreased CD25 expression (IL-2Rα) suggests that the percentage of activated cells diminishes after encountering a local increase in α-syn. However, in PD patients the percentage of cells expressing CD25 within the $CD4^+$ population has been reported to be equal (Baba et al., 2005; Stevens et al., 2012) or increased (Bas et al., 2001; Gruden et al., 2011). Studying the level of CD25 as a function of clinical symptoms or duration of disease might give a clearer answer as to if and how the activated CD4 T cell pool is affected in PD patients. This is important, as IL-2 is necessary for a productive activation of CD4 T cells without which newly activated cells will die. Thus, lack of CD25 expression induced by α-syn could result in the reduced survival capacity of newly activated T cells in PD patients.

Contradictory data has been reported regarding memory CD4+ T cell in PD patients. Stevens et al. reported a decrease in the total number of effector/memory cells, but we found that the percentage within the total CD4 pool appeared increased which is in accordance with other groups (Fiszer et al., 1994; Saunders et al., 2012; Stevens et al., 2012). We observed that fibrillar α-syn reduced CD127 (IL-7Rα) expression which could compromise effector/memory cells survival (or the naïve pool). Indeed, IL-7 signaling inhibits the mitochondrial apoptotic pathway through STAT5 activation (reviewed in Carrette and Surh, 2012). Thus, an explanation for the results observed in PD patients could be that at some stage of PD pathology, when CD4 T cells are exposed to fibrillar α-syn, the effector/memory T cells may die due to lack of IL-7 signaling, resulting in a constant generation of impaired effector/memory cells that in the long run will result in markedly reduced numbers.

http://dx.doi.org/10.1016/j.heliyon.2018.e00513

4.2. Regulatory T cells are regulated by α-syn in a variant-dependent manner

When looking at number and percentage of CD4+Foxp3+ cells, Shameli et al. (2016) showed that α-syn knockout mice have increased CD4+Foxp3+ cells in the spleen, while we show that α-syn and nitrated α-syn do not alter the number of CD4+Foxp3+ cells in LN. Suggesting that α-syn might have a role controlling Treg generation (or at least Foxp3 expression). Interestingly, fibrillar α-syn has the same effect as absence of α-syn, probably indicating that fibrillation does not allow α-syn to sustain its normal functions in T cells and alters their physiology (whereas nitrated α-syn does).

Our data shows that α-syn affected the different Treg compartments in a variant-dependent manner. Monomeric α-syn had a tendency to increase the naïve and activated Treg pools, while the memory pool was significantly contracted; with the concomitant significant reduction of CD127 expression on $CD127^{lo}$ Tregs, which are strongly suppressive (Beyer et al., 2011). Thus, the increase in the naïve/activated Treg pool by monomeric α-syn may be due to the *de novo* generation of highly suppressive Treg. Accordingly, monomeric α-syn increased CD103 expression on Treg, a lectin known to induce cell-cell tolerance.

Nitrated α-syn induced a significant contraction of both the memory and naïve Treg pool, which was reflected in the significant expansion of the activated pool. This could be the result of the activation of the immune system (increased number of CD4+ and CD4− cells) against an allogenic antigen. One could envisage that the immune system would activate the fraction of Tregs specific for the same antigen to prevent autoimmunity. Fibrillar α-syn gave an effect similar to nitrated α-syn, although more potent, reflected by the increased total number of Foxp3+ cells. Indeed, fibrillar α-syn increased the percentage of Foxp3+ cells within the CD4 T cell pool to 80% while reducing their CD25 expression to 20%. This is in agreement with the decreased of the $CD25^{hi}$ fraction of the CD4 pool in PD patients (conventionally considered Treg) (Baba et al., 2005). This decrease of CD25 in the presence of fibrillar α-syn would reduce IL-2 signaling, which could be a mechanism by which: 1) The CD4 T cell pool counteracts its effects rendering the generated Treg cells incapable of surviving (Almeida et al., 2002, 2006), or 2) the CD4 T cells promote generation of inducible Treg cells by limiting IL-2 signaling. Indeed, a low concentration of IL-2 is required to differentiate naïve T cells in the periphery into inducible Treg upon self-antigen encounter (Kretschmer et al., 2005; Zheng et al., 2007). Additionally, Foxp3+CD25− regulatory cells are known to be a reservoir of committed Tregs that are able to express CD25 upon activation (Zelenay et al., 2005) and also to suppress effector cells in an IL-10-dependent manner that does not require cell-cell contacts (Coleman et al., 2012). Furthermore, resting induced Tregs (regulatory cells generated in the periphery)

http://dx.doi.org/10.1016/j.heliyon.2018.e00513

are characterized by being Foxp3+CD25−CD127+ (Li et al., 2011). In PD patient's serum IL-2 was found elevated (Sanchez-Guajardo et al., 2013), but not in *de novo* PD patients (Blum-Degen et al., 1995), suggesting that IL-2 availability increases in later stages of the disease. A third possibility is that, despite Foxp3 expression, the generated cells are not functional. Indeed, *ex vivo* PD-derived Treg (CD4+CD25+CD127−, corresponding to naïve/memory Treg) have lower suppressive activity (Saunders et al., 2012). However, the Treg generated by fibrils were CD25−, which makes us inclined to think that this population is functional.

4.3. α-syn modulates STATs in the CD4 T cell pool in a variant-specific manner

Our results showed that although CD25 expression was downregulated by α-syn, its downstream transcription factor, STAT5, was not. However, STAT3 was significantly decreased by all α-syn variants. STAT3 is the downstream transcription factor of IL-6 signaling, and it is involved in the balance between Foxp3 (Treg) and RORgt (Th17) induction, which is determined by its phosphorylation state. It has been shown that EAE cannot be induced in STAT3-deficient mice (Liu et al., 2008). Likewise, STAT3 affects the generation and maintenance of Treg during challenge with an auto-antigen as absence of STAT3 allows the conversion of naïve CD4 T cells into inducible Tregs in the periphery (Fujino and Li, 2013), and its presence promotes the instability of natural Tregs (produced in the thymus) (Laurence et al., 2012). Thus, the downregulation of STAT3 could be the mechanism by which CD4 T cells are being converted to Foxp3+ cells upon a challenge with fibrillar α-syn.

4.4. Monomeric and nitrated α-syn increase DR-D3 and reduce DR-D2 expression putatively promoting inflammation

Our results showed that monomeric and nitrated α-syn increased DR-D3 while reducing DR-D2 in the CD4 pool. This observation opens up the discussion of the importance of the changes in dopamine availability during PD for T cell biology, as it is well established that dopamine regulates the adaptive immune system (for a review see Pacheco et al., 2010). This is particularly interesting because oxidized dopamine can interact with α-syn resulting in toxic compounds and since dopamine promotes α-syn oligomerization and conversely inhibits the α-syn fibrillization pathway (for a review see Leong et al., 2009). Upregulation of DR-D3 with the concomitant reduction of DR-D2 could signify the induction of a pro-inflammatory state, as DR-D3 signaling in CD4 T cells is associated with inflammation (IFN-γ), while DR-D2 signaling with regulation of immune responses (IL-10) (Pacheco et al., 2009). This Th differentiation dichotomy has been corroborated in animals where absence of DR-D3 in CD4 T cells protects from 1-methyl-4-phenyl-1,2,3,6-

http://dx.doi.org/10.1016/j.heliyon.2018.e00513

tetrahydropyridine (MPTP)-induced neuroinflammation and DR-D2 knockout mice develop PD-like neuroinflammatory features (Pacheco et al., 2014). Indeed, signaling through DR-type-1 (including DR-D1 and DR-D5) induces Th17 responses and the use of antagonists against these receptors prevents Th17 induction (Cosentino et al., 2007; Prado et al., 2012). Monomeric and nitrated α-syn might be promoting an inflammatory CD4 T cell phenotype by acting directly or indirectly on dopamine signaling. The effect of this possible α-syn/dopamine signaling could be very important for understanding how the immune system reacts during PD because with age, α-syn accumulates in healthy human PBMCs; an accumulation that is enhanced in PD patients, compromising cell survival and function (Gardai et al., 2013; Kim et al., 2004). Also, as discussed above, cytokine profiles are not the same in *de novo* PD patients as in treated PD patients (Sanchez-Guajardo et al., 2013), and the susceptibility to oxidative stress observed in PBMCs is reversed with L-DOPA, further suggesting that dopamine signaling on the immune system is also affected during PD and this is detrimental (Battisti et al., 2008; Prigione et al., 2006, 2009).

4.5. Only fibrillar α-syn induces production og anti-α-syn antibodies (IgG)

Anti-α-syn antibodies are found in patients' serum, suggesting a sterile immune response in PD (Besong-Agbo et al., 2013; Maetzler et al., 2011; Papachroni et al., 2007). Additionally, unpublished results from Dr. Sanchez-Guajardo group show in a German cohort of PD patients that the titer of IgG recognizing monomeric α-syn is significantly different in PD patients *vs.* matched controls (*t*-test $p = 0.0386$), and that its titer increases as the UPDRS scores increases (Spearman $r = 0.5358$, $p = 0.0303$) (Tentillier et al., manuscript in preparation). The anti-α-syn antibodies are related to enhance clearance of α-syn in a FcγR-mediated process and results in neuroprotection (Bae et al., 2012, 2013; Masliah et al., 2011). A recent report shows decrease in naturally occurring high affinity autoantibodies against α-syn in PD patients compared to healthy controls, suggesting they could normally have a protective role that weakens in PD patients (Brudek et al., 2017). We observed production of antibodies only in animals injected with fibrillar α-syn. The other forms of α-syn did not induce such increase in antibodies, which might suggest a different B cell response for each type of α-syn, or a higher antigenicity for the fibrillar form of α-syn. The recognition of α-syn-peptides by T-cells in PD patients has been recently reported, supporting specific antigenicity of α-syn (Sulzer et al., 2017).

http://dx.doi.org/10.1016/j.heliyon.2018.e00513

4.6. Microglia respond to peripheral immune changes induced by α-syn

Our findings have shown that events occurring in the periphery can have repercussions in the brain. Despite the lack of α-syn deposition in the brain or microglia proliferation, we did observe molecular expression changes and subtle morphological changes in the microglia upon peripheral challenge with monomeric or nitrated α-syn. Furthermore, microglia in all α-syn groups upregulated CD200R, which would prevent their activation. In animal models of PD, binding to CD200 on neurons prevents microglia activation and dopaminergic neurodegeneration (Zhang et al., 2011). Thus, its upregulation by microglia could be a defense mechanism to prevent the immune system from damaging neurons that naturally express α-syn. Additional surface molecules were as well modulated in an α-syn variant-dependent manner. Monomeric α-syn increased CD103, CD154 and CD54, all endowing microglia with the capacity to interact with T cells in a TCR-independent manner, *i.e.* independently of antigen, and prevent them from becoming activated. Fibrillar α-syn also increased CD154 and CD103, but decreased CD11c. However, nitrated α-syn did not induce any particular polarization and the expression of CD4 and CD11c was decreased. Thus, microglia fine-tuned their phenotypes to adjust to the changes induced in the peripheral immune system. This is not surprising as in PD patients, depending on the disease stage, different cytokines, T cells, and CD68+ microglia have been observed in different brain regions (Garcia-Esparcia et al., 2014), a time and region specificity that has also been observed in PD animal models (Mitra et al., 2011; Watson et al., 2012).

4.7. Peripheral immune changes induced by α-syn also affect the brain

We observed that upon locally increasing α-syn in the periphery, CD4 T cells infiltrated brain parenchyma, but the extent of the infiltration appeared to be variant-dependent. The animals challenged with fibrillar α-syn showed the highest number of infiltrated CD4+ cells, which might suggest that fibrils induces a strong adaptive immune reaction that causes brain surveillance. Nitrated α-syn on the other hand induced the least CD4+ T cell infiltration; nevertheless, this was the only group that showed small round CD4+ cells in contact with microglia. This indicates that only nitrated α-syn might be able to induce a TCR-mediated response, and is supported by the T cell proliferation observed only in this group. In all groups, CD4-expressing microglia were observed in association with blood vessels suggesting a possible crosstalk between brain and periphery, and may further suggest that challenging the peripheral immune system stimulates immunological brain surveillance, and that this response depends on the α-syn variant present. We thus open the possibility that the microglia changes were a response to peripheral immune processes since our histological analysis did not

http://dx.doi.org/10.1016/j.heliyon.2018.e00513

reveal any apparent human α-syn deposition but did show evidence of CD4 T cells and IgG deposition in brain parenchyma 5 days post-injection. However, at this point we cannot ascertain what induced these changes, a direct T or B cell interaction with microglia, or a soluble product such as IgG or cytokines.

5. Conclusion

In conclusion, the adaptive immune system was able to sense local changes to α-syn concentration in a α-syn variant-dependent manner, inducing specific modulation of the CD4+ T cell pool and antibody production. Interestingly, the two pathology-associated variants had very different effects. While nitrated induced expansion of the T cell compartment and direct CD4+ T cell-microglia interactions, fibrils mainly affected Tregs, induced anti-α-syn IgG production, and induced the strongest CD4+ T cell infiltration into brain parenchyma. Hence, how the peripheral adaptive immune system is modulated by α-syn has direct consequences for brain microglia and the ability of the adaptive immune system to access the brain. Thus, potentially during PD, accumulation and modification of α-syn in the periphery will prime and modulate the CD4+ T cell pool, making it able to home into the diseased brain area early on and contribute directly to brain pathology possibly making it worse, or if harnessed, acting as a therapeutic tool.

Declarations

Author contribution statement

Mads N. Olesen, Josefine R. Christiansen: Performed the experiments; Analyzed and interpreted the data.

Steen Vang Petersen: Performed the experiments; Contributed reagents, materials, analysis tools or data.

Poul Henning Jensen, Wojciech Paslawski: Contributed reagents, materials, analysis tools or data.

Marina Romero-Ramos: Analyzed and interpreted the data; Wrote the paper.

Vanesa Sanchez-Guajardo: Conceived and designed the experiments; Analyzed and interpreted the data; Wrote the paper; Performed the experiments.

Competing interest statement

The authors declare no conflict of interest.

http://dx.doi.org/10.1016/j.heliyon.2018.e00513

Funding statement

This work was supported by The Lundbeck Foundation (VSG), Familien Hede Nielsens Fond (VSG), BD Research Grant-Immunology (VSG), and the M. J. Fox Foundation (VSG & MRR).

Additional information

Supplementary content related to this article has been published online at http://dx.doi.org/10.1016/j.heliyon.2018.e00513

Acknowledgements

The authors want to thank Prof. A. A. Freitas (Pasteur Institute, France) for the Foxp3-RFP mice, Dr. D. E. Otzen (iNANO, Department of Molecular Biology and Genetics, Aarhus University) for his invaluable help with the production of α-syn and invaluable support in getting this article published, G. Toft for excellent technical assistance, and the FACS Core Facility at the Department of Biomedicine (Aarhus University) for their invaluable assistance and support.

References

Almeida, A.R., Legrand, N., Papiernik, M., Freitas, A.A., 2002. Homeostasis of peripheral CD4+ T cells: IL-2R alpha and IL-2 shape a population of regulatory cells that controls CD4+ T cell numbers. J. Immunol. 169 (9), 4850–4860.

Almeida, A.R., Zaragoza, B., Freitas, A.A., 2006. Indexation as a novel mechanism of lymphocyte homeostasis: the number of CD4+CD25+ regulatory T cells is indexed to the number of IL-2-producing cells. J. Immunol. 177 (1), 192–200.

Baba, Y., Kuroiwa, A., Uitti, R.J., Wszolek, Z.K., Yamada, T., 2005. Alterations of T-lymphocyte populations in Parkinson disease. Parkinsonism Relat. Disord. 11 (8), 493–498.

Bae, E.J., Ho, D.H., Park, E., Jung, J.W., Cho, K., Hong, J.H., Lee, S.J., 2013. Lipid peroxidation product 4-hydroxy-2-nonenal promotes seeding-capable oligomer formation and cell-to-cell transfer of alpha-synuclein. Antioxid. Redox Signal. 18 (7), 770–783.

Bae, E.J., Lee, H.J., Rockenstein, E., Ho, D.H., Park, E.B., Yang, N.Y., Lee, S.J., 2012. Antibody-aided clearance of extracellular alpha-synuclein prevents cell-to-cell aggregate transmission. J. Neurosci. 32 (39), 13454–13469.

Barbour, R., Kling, K., Anderson, J.P., Banducci, K., Cole, T., Diep, L., Chilcote, T.J., 2008. Red blood cells are the major source of alpha-synuclein in blood. Neurodegener. Dis. 5 (2), 55–59.

Barkholt, P., Sanchez-Guajardo, V., Kirik, D., Romero-Ramos, M., 2012. Long-term polarization of microglia upon alpha-synuclein overexpression in nonhuman primates. Neuroscience 208, 85–96.

Bas, J., Calopa, M., Mestre, M., Mollevi, D.G., Cutillas, B., Ambrosio, S., Buendia, E., 2001. Lymphocyte populations in Parkinson's disease and in rat models of Parkinsonism. J. Neuroimmunol. 113 (1), 146–152.

Battisti, C., Formichi, P., Radi, E., Federico, A., 2008. Oxidative-stress-induced apoptosis in PBLs of two patients with Parkinson disease secondary to alpha-synuclein mutation. J. Neurol. Sci. 267 (1–2), 120–124.

Beatman, E.L., Massey, A., Shives, K.D., Burrack, K.S., Chamanian, M., Morrison, T.E., Beckham, J.D., 2015. Alpha-synuclein expression restricts RNA viral infections in the brain. J. Virol. 90 (6), 2767–2782.

Besong-Agbo, D., Wolf, E., Jessen, F., Oechsner, M., Hametner, E., Poewe, W., Dodel, R., 2013. Naturally occurring alpha-synuclein autoantibody levels are lower in patients with Parkinson disease. Neurology 80 (2), 169–175.

Beyer, M., Classen, S., Endl, E., Kochanek, M., Weihrauch, M.R., Debey-Pascher, S., Schultze, J.L., 2011. Comparative approach to define increased regulatory T cells in different cancer subtypes by combined assessment of CD127 and FOXP3. Clin. Dev. Immunol 734036.

Blum-Degen, D., Muller, T., Kuhn, W., Gerlach, M., Przuntek, H., Riederer, P., 1995. Interleukin-1 beta and interleukin-6 are elevated in the cerebrospinal fluid of Alzheimer's and de novo Parkinson's disease patients. Neurosci. Lett. 202 (1–2), 17–20.

Brochard, V., Combadiere, B., Prigent, A., Laouar, Y., Perrin, A., Beray-Berthat, V., Hunot, S., 2009. Infiltration of CD4+ lymphocytes into the brain contributes to neurodegeneration in a mouse model of Parkinson disease. J. Clin. Invest. 119 (1), 182–192.

Brudek, T., Winge, K., Folke, J., Christensen, S., Fog, K., Pakkenberg, B., Pedersen, L.O., 2017. Autoimmune antibody decline in Parkinson's disease and Multiple System Atrophy; a step towards immunotherapeutic strategies. Mol. Neurodegener. 12 (1), 44.

Cappai, R., Leck, S.L., Tew, D.J., Williamson, N.A., Smith, D.P., Galatis, D., Hill, A.F., 2005. Dopamine promotes alpha-synuclein aggregation into SDS-resistant soluble oligomers via a distinct folding pathway. Faseb J. 19 (10), 1377–1379.

Carrette, F., Surh, C.D., 2012. IL-7 signaling and CD127 receptor regulation in the control of T cell homeostasis. Semin. Immunol. 24 (3), 209–217.

 http://dx.doi.org/10.1016/j.heliyon.2018.e00513

Castano, A., Herrera, A.J., Cano, J., Machado, A., 2002. The degenerative effect of a single intranigral injection of LPS on the dopaminergic system is prevented by dexamethasone, and not mimicked by rh-TNF-alpha, IL-1beta and IFN-gamma. J. Neurochem. 81 (1), 150–157.

Coleman, M.M., Finlay, C.M., Moran, B., Keane, J., Dunne, P.J., Mills, K.H., 2012. The immunoregulatory role of CD4(+) FoxP3(+) CD25(−) regulatory T cells in lungs of mice infected with Bordetella pertussis. FEMS Immunol. Med. Microbiol. 64 (3), 413–424.

Conway, K.A., Rochet, J.C., Bieganski, R.M., Lansbury Jr., P.T., 2001. Kinetic stabilization of the alpha-synuclein protofibril by a dopamine-alpha-synuclein adduct. Science 294 (5545), 1346–1349.

Cosentino, M., Fietta, A.M., Ferrari, M., Rasini, E., Bombelli, R., Carcano, E., Lecchini, S., 2007. Human CD4+CD25+ regulatory T cells selectively express tyrosine hydroxylase and contain endogenous catecholamines subserving an autocrine/paracrine inhibitory functional loop. Blood 109 (2), 632–642.

Desplats, P., Lee, H.J., Bae, E.J., Patrick, C., Rockenstein, E., Crews, L., Lee, S.J., 2009. Inclusion formation and neuronal cell death through neuron-to-neuron transmission of alpha-synuclein. Proc. Natl. Acad. Sci. U. S. A. 106 (31), 13010–13015.

Fiszer, U., Mix, E., Fredrikson, S., Kostulas, V., Link, H., 1994. Parkinson's disease and immunological abnormalities: increase of HLA-DR expression on monocytes in cerebrospinal fluid and of CD45RO+ T cells in peripheral blood. Acta Neurol. Scand. 90 (3), 160–166.

Fujino, M., Li, X.K., 2013. Role of STAT3 in regulatory T lymphocyte plasticity during acute graft-vs.-host-disease. Jakstat 2 (4), e24529.

Gao, H.M., Zhang, F., Zhou, H., Kam, W., Wilson, B., Hong, J.S., 2011. Neuroinflammation and alpha-synuclein dysfunction potentiate each other, driving chronic progression of neurodegeneration in a mouse model of Parkinson's disease. Environ. Health Perspect. 119 (6), 807–814.

Garcia-Esparcia, P., Llorens, F., Carmona, M., Ferrer, I., 2014. Complex deregulation and expression of cytokines and mediators of the immune response in Parkinson's disease brain is region dependent. Brain Pathol. 24 (6), 584–598.

Gardai, S.J., Mao, W., Schule, B., Babcock, M., Schoebel, S., Lorenzana, C., Johnston, J.A., 2013. Elevated alpha-synuclein impairs innate immune cell function and provides a potential peripheral biomarker for Parkinson's disease. PLoS One 8 (8), e71634.

http://dx.doi.org/10.1016/j.heliyon.2018.e00513

Goedert, M., 2015. Neurodegeneration. Alzheimer's and Parkinson's diseases: the prion concept in relation to assembled Abeta, tau, and alpha-synuclein. Science 349 (6248).

Gonzalez, H., Contreras, F., Prado, C., Elgueta, D., Franz, D., Bernales, S., Pacheco, R., 2013. Dopamine receptor D3 expressed on CD4+ T cells favors neurodegeneration of dopaminergic neurons during Parkinson's disease. J. Immunol. 190 (10), 5048–5056.

Grabert, K., Michoel, T., Karavolos, M.H., Clohisey, S., Baillie, J.K., Stevens, M.P., McColl, B.W., 2016. Microglial brain region-dependent diversity and selective regional sensitivities to aging. Nat. Neurosci. 19 (3), 504–516.

Gruden, M.A., Sewell, R.D., Yanamandra, K., Davidova, T.V., Kucheryanu, V.G., Bocharov, E.V., Morozova-Roche, L.A., 2011. Immunoprotection against toxic biomarkers is retained during Parkinson's disease progression. J. Neuroimmunol. 233 (1–2), 221–227.

Hisanaga, K., Asagi, M., Itoyama, Y., Iwasaki, Y., 2001. Increase in peripheral CD4 bright+CD8 dull+ T cells in Parkinson disease. Arch. Neurol. 58 (10), 1580–1583.

Huang, G., Wang, Y., Chi, H., 2013. Control of T cell fates and immune tolerance by p38alpha signaling in mucosal CD103+ dendritic cells. J. Immunol. 191 (2), 650–659.

Kim, S., Jeon, B.S., Heo, C., Im, P.S., Ahn, T.B., Seo, J.H., Suh, Y.H., 2004. Alpha-synuclein induces apoptosis by altered expression in human peripheral lymphocyte in Parkinson's disease. FASEB J. 18 (13), 1615–1617.

Kretschmer, K., Apostolou, I., Hawiger, D., Khazaie, K., Nussenzweig, M.C., von Boehmer, H., 2005. Inducing and expanding regulatory T cell populations by foreign antigen. Nat. Immunol. 6 (12), 1219–1227.

Kustrimovic, N., Rasini, E., Legnaro, M., Bombelli, R., Aleksic, I., Blandini, F., Cosentino, M., 2016. Dopaminergic receptors on CD4+ T naive and memory lymphocytes correlate with motor impairment in patients with Parkinson's disease. Sci. Rep. 6, 33738.

Laurence, A., Amarnath, S., Mariotti, J., Kim, Y.C., Foley, J., Eckhaus, M., Fowler, D.H., 2012. STAT3 transcription factor promotes instability of nTreg cells and limits generation of iTreg cells during acute murine graft-versus-host disease. Immunity 37 (2), 209–222.

Lee, H.J., Baek, S.M., Ho, D.H., Suk, J.E., Cho, E.D., Lee, S.J., 2011. Dopamine promotes formation and secretion of non-fibrillar alpha-synuclein oligomers. Exp. Mol. Med. 43 (4), 216–222.

 http://dx.doi.org/10.1016/j.heliyon.2018.e00513

Lee, P.H., Lee, G., Park, H.J., Bang, O.Y., Joo, I.S., Huh, K., 2006. The plasma alpha-synuclein levels in patients with Parkinson's disease and multiple system atrophy. J. Neural Transm. (Vienna) 113 (10), 1435–1439.

Lee, S.J., Desplats, P., Lee, H.J., Spencer, B., Masliah, E., 2012. Cell-to-cell transmission of alpha-synuclein aggregates. Methods Mol. Biol. 849, 347–359.

Leong, S.L., Cappai, R., Barnham, K.J., Pham, C.L., 2009. Modulation of alpha-synuclein aggregation by dopamine: a review. Neurochem. Res. 34 (10), 1838–1846.

Li, C.R., Deiro, M.F., Godebu, E., Bradley, L.M., 2011. IL-7 uniquely maintains FoxP3(+) adaptive Treg cells that reverse diabetes in NOD mice via integrin-beta7-dependent localization. J. Autoimmun. 37 (3), 217–227.

Lindersson, E., Beedholm, R., Hojrup, P., Moos, T., Gai, W., Hendil, K.B., Jensen, P.H., 2004. Proteasomal inhibition by alpha-synuclein filaments and oligomers. J. Biol. Chem. 279 (13), 12924–12934.

Liu, X., Lee, Y.S., Yu, C.R., Egwuagu, C.E., 2008. Loss of STAT3 in CD4+ T cells prevents development of experimental autoimmune diseases. J. Immunol. 180 (9), 6070–6076.

Luk, K.C., Kehm, V., Carroll, J., Zhang, B., O'Brien, P., Trojanowski, J.Q., Lee, V. M., 2012. Pathological alpha-synuclein transmission initiates Parkinson-like neurodegeneration in nontransgenic mice. Science 338 (6109), 949–953.

Maetzler, W., Berg, D., Synofzik, M., Brockmann, K., Godau, J., Melms, A., Langkamp, M., 2011. Autoantibodies against amyloid and glial-derived antigens are increased in serum and cerebrospinal fluid of Lewy body-associated dementias. J. Alzheimers Dis. 26 (1), 171–179.

Masliah, E., Rockenstein, E., Mante, M., Crews, L., Spencer, B., Adame, A., Schenk, D., 2011. Passive immunization reduces behavioral and neuropathological deficits in an alpha-synuclein transgenic model of Lewy body disease. PLoS One 6 (4) e19338.

Mitra, S., Chakrabarti, N., Bhattacharyya, A., 2011. Differential regional expression patterns of alpha-synuclein, TNF-alpha, and IL-1beta; and variable status of dopaminergic neurotoxicity in mouse brain after paraquat treatment. J. Neuroinflamm. 8, 163.

Mollenhauer, B., 2014. Quantification of alpha-synuclein in cerebrospinal fluid: how ideal is this biomarker for Parkinson's disease? Parkinsonism Relat. Disord. 20 (Suppl. 1), S76–S79.

 http://dx.doi.org/10.1016/j.heliyon.2018.e00513

Nagai, Y., Ueno, S., Saeki, Y., Soga, F., Hirano, M., Yanagihara, T., 1996. Decrease of the D3 dopamine receptor mRNA expression in lymphocytes from patients with Parkinson's disease. Neurology 46 (3), 791–795.

Nielsen, S.B., Macchi, F., Raccosta, S., Langkilde, A.E., Giehm, L., Kyrsting, A., Otzen, D.E., 2013. Wildtype and A30 P mutant alpha-synuclein form different fibril structures. PLoS One 8 (7), e67713.

Outeiro, T.F., Klucken, J., Bercury, K., Tetzlaff, J., Putcha, P., Oliveira, L.M., Hyman, B.T., 2009. Dopamine-induced conformational changes in alpha-synuclein. PLoS One 4 (9), e6906.

Pacheco, R., Contreras, F., Zouali, M., 2014. The dopaminergic system in autoimmune diseases. Front. Immunol. 5, 117.

Pacheco, R., Prado, C.E., Barrientos, M.J., Bernales, S., 2009. Role of dopamine in the physiology of T-cells and dendritic cells. J. Neuroimmunol. 216 (1–2), 8–19.

Pacheco, R., Riquelme, E., Kalergis, A.M., 2010. Emerging evidence for the role of neurotransmitters in the modulation of T cell responses to cognate ligands. Cent. Nerv. Syst. Agents Med. Chem. 10 (1), 65–83.

Papachroni, K.K., Ninkina, N., Papapanagiotou, A., Hadjigeorgiou, G.M., Xiromerisiou, G., Papadimitriou, A., Buchman, V.L., 2007. Autoantibodies to alpha-synuclein in inherited Parkinson's disease. J. Neurochem. 101 (3), 749–756.

Prado, C., Contreras, F., Gonzalez, H., Diaz, P., Elgueta, D., Barrientos, M., Pacheco, R., 2012. Stimulation of dopamine receptor D5 expressed on dendritic cells potentiates Th17-mediated immunity. J. Immunol. 188 (7), 3062–3070.

Prigione, A., Begni, B., Galbussera, A., Beretta, S., Brighina, L., Garofalo, R., Ferrarese, C., 2006. Oxidative stress in peripheral blood mononuclear cells from patients with Parkinson's disease: negative correlation with levodopa dosage. Neurobiol. Dis. 23 (1), 36–43.

Prigione, A., Isaias, I.U., Galbussera, A., Brighina, L., Begni, B., Andreoni, S., Ferrarese, C., 2009. Increased oxidative stress in lymphocytes from untreated Parkinson's disease patients. Parkinsonism Relat. Disord. 15 (4), 327–328.

Reboldi, A., Coisne, C., Baumjohann, D., Benvenuto, F., Bottinelli, D., Lira, S., Sallusto, F., 2009. C-C chemokine receptor 6-regulated entry of TH-17 cells into the CNS through the choroid plexus is required for the initiation of EAE. Nat. Immunol. 10 (5), 514–523.

Reynolds, A.D., Stone, D.K., Hutter, J.A., Benner, E.J., Mosley, R.L., Gendelman, H.E., 2010. Regulatory T cells attenuate Th17 cell-mediated nigrostriatal

 http://dx.doi.org/10.1016/j.heliyon.2018.e00513

dopaminergic neurodegeneration in a model of Parkinson's disease. J. Immunol. 184 (5), 2261–2271.

Rosenkranz, D., Weyer, S., Tolosa, E., Gaenslen, A., Berg, D., Leyhe, T., Stoltze, L., 2007. Higher frequency of regulatory T cells in the elderly and increased suppressive activity in neurodegeneration. J. Neuroimmunol. 188 (1–2), 117–127.

Saha, B., Mondal, A.C., Majumder, J., Basu, S., Dasgupta, P.S., 2001. Physiological concentrations of dopamine inhibit the proliferation and cytotoxicity of human CD4+ and CD8+ T cells in vitro: a receptor-mediated mechanism. Neuroimmunomodulation 9 (1), 23–33.

Sanchez-Guajardo, V., Barnum, C.J., Tansey, M.G., Romero-Ramos, M., 2013. Neuroimmunological processes in Parkinson's disease and their relation to alpha-synuclein: microglia as the referee between neuronal processes and peripheral immunity. ASN Neuro 5 (2), 113–139.

Sanchez-Guajardo, V., Febbraro, F., Kirik, D., Romero-Ramos, M., 2010. Microglia acquire distinct activation profiles depending on the degree of alpha-synuclein neuropathology in a rAAV based model of Parkinson's disease. PLoS One 5 (1), e8784.

Saunders, J.A., Estes, K.A., Kosloski, L.M., Allen, H.E., Dempsey, K.M., Torres-Russotto, D.R., Gendelman, H.E., 2012. CD4+ regulatory and effector/memory T cell subsets profile motor dysfunction in Parkinson's disease. J. Neuroimmune Pharmacol. 7 (4), 927–938.

Schonbeck, U., Libby, P., 2001. The CD40/CD154 receptor/ligand dyad. Cell Mol. Life Sci. 58 (1), 4–43.

Shameli, A., Xiao, W., Zheng, Y., Shyu, S., Sumodi, J., Meyerson, H.J., Maitta, R. W., 2016. A critical role for alpha-synuclein in development and function of T lymphocytes. Immunobiology 221 (2), 333–340.

Shin, E.C., Cho, S.E., Lee, D.K., Hur, M.W., Paik, S.R., Park, J.H., Kim, J., 2000. Expression patterns of alpha-synuclein in human hematopoietic cells and in Drosophila at different developmental stages. Mol. Cells 10 (1), 65–70.

Stevens, C.H., Rowe, D., Morel-Kopp, M.C., Orr, C., Russell, T., Ranola, M., Halliday, G.M., 2012. Reduced T helper and B lymphocytes in Parkinson's disease. J. Neuroimmunol. 252 (1–2), 95–99.

Sulzer, D., Alcalay, R.N., Garretti, F., Cote, L., Kanter, E., Agin-Liebes, J., Sette, A., 2017. T cells from patients with Parkinson's disease recognize alpha-synuclein peptides. Nature 546 (7660), 656–661.

 http://dx.doi.org/10.1016/j.heliyon.2018.e00513

Tinsley, R.B., Bye, C.R., Parish, C.L., Tziotis-Vais, A., George, S., Culvenor, J.G., Horne, M.K., 2009. Dopamine D2 receptor knockout mice develop features of Parkinson disease. Ann. Neurol. 66 (4), 472–484.

Wan, Y.Y., Flavell, R.A., 2005. Identifying Foxp3-expressing suppressor T cells with a bicistronic reporter. Proc. Natl. Acad. Sci. U. S. A. 102 (14), 5126–5131.

Wang, L., Xie, Y., Zhu, L.J., Chang, T.T., Mao, Y.Q., Li, J., 2010. An association between immunosenescence and CD4(+)CD25(+) regulatory T cells: a systematic review. Biomed. Environ. Sci. 23 (4), 327–332.

Waters, W.R., Rahner, T.E., Palmer, M.V., Cheng, D., Nonnecke, B.J., Whipple, D.L., 2003. Expression of L-selectin (CD62L), CD44, and CD25 on activated bovine T cells. Infect. Immun. 71 (1), 317–326.

Watson, M.B., Richter, F., Lee, S.K., Gabby, L., Wu, J., Masliah, E., Chesselet, M. F., 2012. Regionally-specific microglial activation in young mice over-expressing human wildtype alpha-synuclein. Exp. Neurol. 237 (2), 318–334.

Xiao, W., Shameli, A., Harding, C.V., Meyerson, H.J., Maitta, R.W., 2014. Late stages of hematopoiesis and B cell lymphopoiesis are regulated by alpha-synuclein, a key player in Parkinson's disease. Immunobiology 219 (11), 836–844.

Zelenay, S., Lopes-Carvalho, T., Caramalho, I., Moraes-Fontes, M.F., Rebelo, M., Demengeot, J., 2005. Foxp3+ CD25− CD4 T cells constitute a reservoir of committed regulatory cells that regain CD25 expression upon homeostatic expansion. Proc. Natl. Acad. Sci. U. S. A. 102 (11), 4091–4096.

Zhang, S., Wang, X.J., Tian, L.P., Pan, J., Lu, G.Q., Zhang, Y.J., Chen, S.D., 2011. CD200-CD200R dysfunction exacerbates microglial activation and dopaminergic neurodegeneration in a rat model of Parkinson's disease. J. Neuroinflamm. 8, 154.

Zheng, S.G., Wang, J., Wang, P., Gray, J.D., Horwitz, D.A., 2007. IL-2 is essential for TGF-beta to convert naive CD4+CD25− cells to CD25+Foxp3+ regulatory T cells and for expansion of these cells. J. Immunol. 178 (4), 2018–2027.

http://dx.doi.org/10.1016/j.heliyon.2018.e00513